AMERICAN SOCIETY FOR MICROBIOLOGY | Infection and Immunity®

BACTERIAL INFECTIONS

Acinetobacter baumannii OxyR Regulates the Transcriptional Response to Hydrogen Peroxide

Lillian J. Juttukonda,[a,b] Erin R. Green,[a,b] Zachery R. Lonergan,[a,b] Marie C. Heffern,[c*] Christopher J. Chang,[c,d,e] Eric P. Skaar[a,b]

[a]Vanderbilt Institute for Infection, Immunology, and Inflammation, Vanderbilt University Medical Center, Nashville, Tennessee, USA
[b]Department of Pathology, Microbiology, and Immunology, Vanderbilt University Medical Center, Nashville, Tennessee, USA
[c]Department of Chemistry, University of California, Berkeley, California, USA
[d]Department of Molecular and Cell Biology, University of California, Berkeley, California, USA
[e]Howard Hughes Medical Institute, University of California, Berkeley, California, USA

ABSTRACT *Acinetobacter baumannii* is a Gram-negative opportunistic pathogen that causes diverse infections, including pneumonia, bacteremia, and wound infections. Due to multiple intrinsic and acquired antimicrobial-resistance mechanisms, *A. baumannii* isolates are commonly multidrug resistant, and infections are notoriously difficult to treat. The World Health Organization recently highlighted carbapenem-resistant *A. baumannii* as a "critical priority" for the development of new antimicrobials because of the risk to human health posed by this organism. Therefore, it is important to discover the mechanisms used by *A. baumannii* to survive stresses encountered during infection in order to identify new drug targets. In this study, by use of *in vivo* imaging, we identified hydrogen peroxide (H_2O_2) as a stressor produced in the lung during *A. baumannii* infection and defined OxyR as a transcriptional regulator of the H_2O_2 stress response. Upon exposure to H_2O_2, *A. baumannii* differentially transcribes several hundred genes. However, the transcriptional upregulation of genes predicted to detoxify hydrogen peroxide is abolished in an *A. baumannii* strain in which the transcriptional regulator *oxyR* is genetically inactivated. Moreover, inactivation of *oxyR* in both antimicrobial-susceptible and multidrug-resistant *A. baumannii* strains impairs growth in the presence of H_2O_2. OxyR is a direct regulator of *katE* and *ahpF1*, which encode the major H_2O_2-degrading enzymes in *A. baumannii*, as confirmed through measurement of promoter binding by recombinant OxyR in electromobility shift assays. Finally, an *oxyR* mutant is less fit than wild-type *A. baumannii* during infection of the murine lung. This work reveals a mechanism used by this important human pathogen to survive H_2O_2 stress encountered during infection.

KEYWORDS *Acinetobacter baumannii*, hydrogen peroxide, OxyR, RNA sequencing, *in vivo* imaging, transcriptional regulation

Acinetobacter baumannii is a Gram-negative coccobacillus and an obligate aerobe. *A. baumannii* is best known as an agent of ventilator-associated pneumonia and bloodstream infections in critically ill patients but also causes hospital-acquired infections of virtually any body site, including skin and soft tissue infections, wound infections, urinary tract infections, and meningitis (1, 2). Since the original recognition of *A. baumannii* as a frequent opportunistic pathogen, this organism has emerged as one of the most difficult bacterial infectious agents to treat because of extensive intrinsic and evolved antimicrobial resistance (1, 3–6). Globally, 63% of *A. baumannii* isolates were found to be multidrug resistant in 2014, an increase from 23% in 2004 (7). In particular, the threat to global human health from increasing rates of carbapenem-resistant *A. baumannii* infections has led the World Health Organization to name

Citation Juttukonda LJ, Green ER, Lonergan ZR, Heffern MC, Chang CJ, Skaar EP. 2019. *Acinetobacter baumannii* OxyR regulates the transcriptional response to hydrogen peroxide. Infect Immun 87:e00413-18. https://doi.org/10.1128/IAI.00413-18.

Editor Marvin Whiteley, Georgia Institute of Technology School of Biological Sciences

Address correspondence to Eric P. Skaar, eric.skaar@vumc.org.

* Present address: Marie C. Heffern, Department of Chemistry, University of California, Davis, California, USA.

Received 24 May 2018
Returned for modification 2 July 2018
Accepted 3 October 2018

Accepted manuscript posted online 8 October 2018
Published 19 December 2018

carbapenem-resistant *A. baumannii* the number one "critical" priority for the development of new antibiotics (8). Therefore, research investigating mechanisms by which *A. baumannii* survives within hosts and in the environment is urgently needed as a strategy to identify new targets for therapeutic intervention.

A. baumannii does not typically use classical virulence determinants such as effector toxins or immune evasion strategies (3, 9). Instead, *A. baumannii* utilizes genes that have evolved for survival in the environment to persist during infection (9, 10). Moreover, the ability of *A. baumannii* to survive within the hospital environment permits this organism to cause outbreaks of hospital-associated infections that are difficult to eradicate (11). We therefore predict that processes involved in sensing and responding to the environment are critical for *A. baumannii* to be a successful opportunistic pathogen.

During infection, bacteria experience numerous stresses imposed by the host. One stress thought to be encountered during infection is reactive oxygen species produced by effector cells of the innate immune system (12). Neutrophils treated with various proinflammatory stimuli *ex vivo* generate an oxidative burst initiated by NADPH phagocyte oxidase that results in the production of superoxide, H_2O_2, hypochlorous acid, and peroxynitrate (12). Mice lacking NADPH phagocyte oxidase are more susceptible to *A. baumannii* pneumonia (13). Therefore, we hypothesized that H_2O_2 is formed in the lung during *A. baumannii* pneumonia and thus is a stress that *A. baumannii* must overcome in order to survive and infect the lung.

Bacteria have evolved mechanisms to sense damaging molecules and induce an appropriate transcriptional response, such as upregulation of enzymes that detoxify reactive oxygen species. Transcriptional regulators that sense either the reactive molecule itself or the damage caused by reactive molecules control the production of detoxification proteins (14). H_2O_2 is detoxified by alkyl hydroperoxide reductase (Ahp) and catalase (Kat), which reduce H_2O_2 to water (15). In *A. baumannii*, the catalase genes *katE* and *katG* and the universal stress protein UspA protect against H_2O_2 stress (16, 17). However, the regulatory mechanisms that govern the transcriptional response of *A. baumannii* to H_2O_2 have not been characterized.

In Gram-negative bacteria, OxyR is the canonical orchestrator of the H_2O_2 detoxification response (18). OxyR is a highly conserved transcriptional regulator of the LysR family that senses and responds to H_2O_2 stress (19–21). Oxidation of a conserved cysteine residue causes OxyR to undergo a conformational change, resulting in altered DNA binding (21–25). In *Escherichia coli*, OxyR serves as a transcriptional activator of genes involved in H_2O_2 detoxification, including *ahp*, which encodes alkyl hydroperoxide reductase; *kat*, which encodes catalase; and *dps*, which encodes a protein for DNA protection during starvation (19, 26). While OxyR is highly conserved, the function of this protein differs between organisms. For instance, while OxyR is classically described as a transcriptional activator, OxyR in *Corynebacterium glutamicum* is a transcriptional repressor, and inactivation of *oxyR* enhances resistance to H_2O_2 in this organism (27). There are also discrepancies regarding the sensitivity of *oxyR* mutants to H_2O_2 killing during log-phase growth. *Xanthomonas campestris* lacking *oxyR* is sensitive to H_2O_2 during log-phase growth, but *Neisseria meningitidis* and *Brucella abortus* inactivated for *oxyR* are resistant to H_2O_2 killing in exponential growth (28–30). While *oxyR* homologues in *A. baumannii* and other *Acinetobacter* species have been identified and shown to confer resistance to H_2O_2 on agar plates, the functional role of *A. baumannii* OxyR in transcriptional regulation and survival *in vivo* has not been studied (31–33).

We hypothesized that *A. baumannii* encounters H_2O_2 stress during infection and that OxyR controls the transcriptional response to this stress. In this study, we demonstrate that H_2O_2 is formed during *A. baumannii* infection of the lung, and we characterize the transcriptional response of *A. baumannii* to H_2O_2 by RNA sequencing. Furthermore, we define the role of *A. baumannii oxyR* in defense against H_2O_2 stress, determine the regulon of OxyR by RNA sequencing, and confirm direct promoter binding by recombinant OxyR. Finally, we study the role of *oxyR* in *A. baumannii* infection of the murine lung. By identifying the role and regulon of OxyR in *A.*

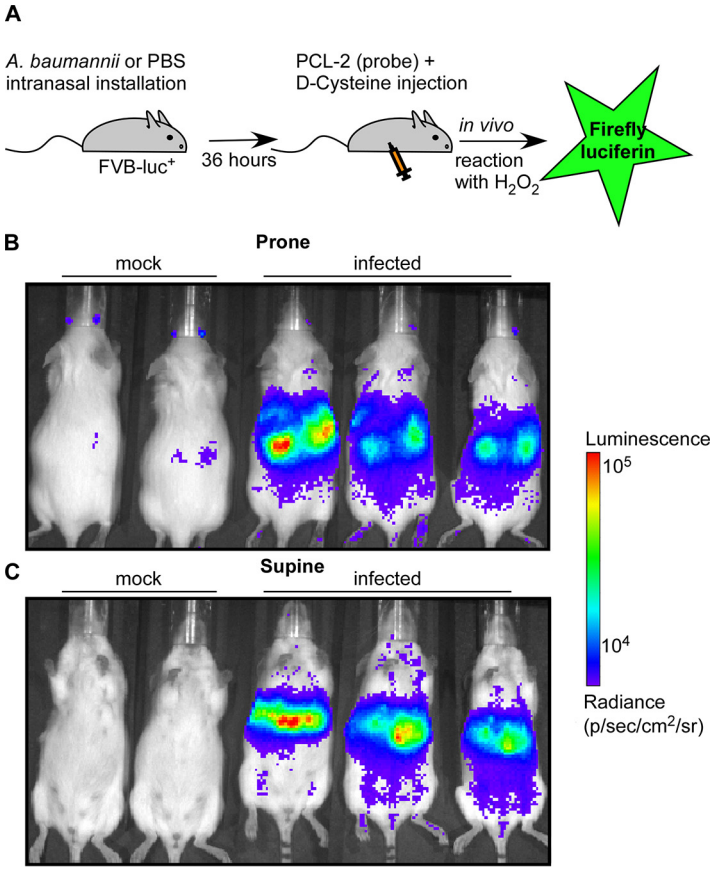

FIG 1 H_2O_2 is produced during *A. baumannii* lung infection. (A) Schematic of the experimental design. Mice were either infected with WT *A. baumannii* or mock infected with PBS. Imaging was performed 36 h postinfection. The production of H_2O_2 was monitored *in vivo* by injection of a caged luciferin probe (PCL-2) that specifically reacts with H_2O_2 to generate bioluminescence (35). (B and C) Mice were placed in the prone position (B) and in the supine position (C). The results are representative of two independent experiments.

baumannii, we have defined a transcriptional regulatory network in this important human pathogen that confers resistance to the stresses it encounters during infection. These findings provide a foundation for the development of novel therapeutics against *A. baumannii* infections.

RESULTS

***A. baumannii* lung infection induces H_2O_2 production.** H_2O_2 is produced by the neutrophil oxidative burst (12), and neutrophils are recruited in response to *A. baumannii* infection (34). In order to test our hypothesis that H_2O_2 functions as an antimicrobial during *A. baumannii* lung infection, we first wanted to determine if we could directly visualize H_2O_2 production *in vivo*. Thus, we employed a recently developed bioluminescence system in which a caged luciferin probe specifically reacts with H_2O_2 to release D-luciferin, which leads to bioluminescence in mice that constitutively express luciferase (Fig. 1A) (35, 36). Upon intranasal inoculation with *A. baumannii* ATCC 17978, substantial bioluminescence was detected in the thoracic cavity, whereas minimal bioluminescence was detected following mock infection with phosphate-buffered saline (PBS) (Fig. 1B and C). Based on these data, we conclude that infection with *A. baumannii* stimulates the production of H_2O_2 in the lung.

H_2O_2 exposure alters the transcriptome of *A. baumannii* in an *oxyR*-dependent manner. Considering the success of *A. baumannii* as a pathogen, this organism must survive an onslaught of H_2O_2 produced *in vivo*. The mechanisms by which *A. baumannii* defends against H_2O_2 are not defined. We characterized the response of *A. baumannii*

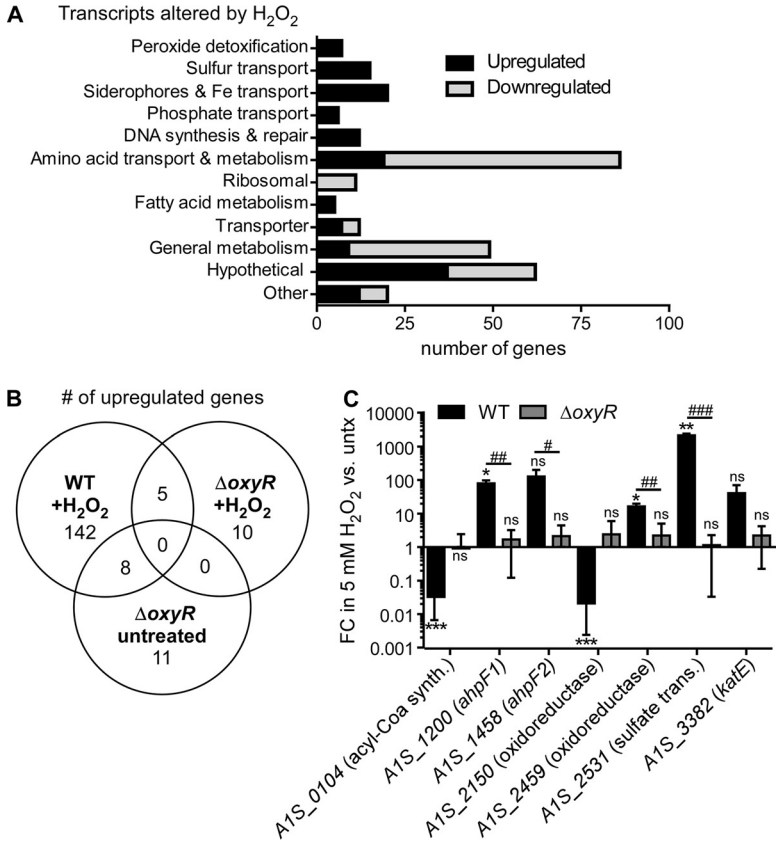

FIG 2 H_2O_2 exposure alters the transcriptome of *A. baumannii* in an *oxyR*-dependent manner. (A to C) RNA sequencing was performed on RNA extracted from WT *A. baumannii* and the Δ*oxyR* strain, which were grown to mid-exponential phase and treated with 5 mM H_2O_2 for 10 min. (A) Classification of transcripts significantly up- or downregulated in WT *A. baumannii* treated with H_2O_2 relative to expression in untreated cells (>2 $\log_2$-fold change; P, <0.05, corrected for the FDR). (B) Venn diagram comparing common upregulated transcripts under the following conditions: the WT strain plus H_2O_2 (relative to the untreated WT strain), the Δ*oxyR* strain plus H_2O_2 (relative to the untreated Δ*oxyR* strain), and the untreated Δ*oxyR* strain (relative to the untreated WT strain). (C) Validation of selected RNA sequencing results by qRT-PCR in WT *A. baumannii* and the Δ*oxyR* strain treated with H_2O_2. Results are depicted as the fold change (FC) in gene transcript abundance following a 10-min treatment with 5 mM H_2O_2 relative to no treatment (untx). *, $P < 0.05$; **, $P < 0.01$; ***, $P < 0.001$ (by *t* test against a theoretical value of 1.0). #, $P < 0.05$; ##, $P < 0.01$; ###, $P < 0.001$ (by a *t* test comparing the WT and the Δ*oxyR* strain). Results are means ± standard deviations for three biological replicates.

to H_2O_2 exposure by RNA sequencing. Compared to mock-treated cells, cells exposed to H_2O_2 upregulated the transcription of 155 genes and downregulated the transcription of 151 genes (Fig. 2A and B; Table 1; see also Table S2 in the supplemental material). Genes encoding proteins that directly detoxify H_2O_2, including *ahpF1* (*A1S_1200–1201*), *ahpF2* (*A1S_1458–1460*), and *katE* (*A1S_3382*), were strongly upregulated. Genes involved in sulfur transport and iron homeostasis were also highly upregulated by H_2O_2 exposure, which we postulate occurs in response to the oxidation of iron-sulfur (Fe-S) clusters by H_2O_2 (15). Amino acid transport and metabolism pathways were also upregulated by H_2O_2, perhaps as a repair or replacement mechanism for proteins that sustained oxidative damage. *A. baumannii* also increases the transcription of phosphate transport and nucleic acid synthesis and repair genes, a response consistent with H_2O_2-induced DNA damage (15). Treatment with H_2O_2 predominantly downregulates metabolic and synthetic genes, suggesting a model in which most cellular metabolism is paused while the acute toxicity is managed (Table S2 in the supplemental material).

Many Gram-negative organisms defend against H_2O_2 by inducing the OxyR regulon, which includes genes encoding the H_2O_2-reducing enzymes catalase and alkyl hy-

TABLE 1 Genes with increased expression in WT *A. baumannii* following treatment with H_2O_2

Category and locus	Annotation (KEGG)[a]	Fold change
Peroxide detoxification		
A1S_1459	Alkyl hydroperoxide reductase subunit F (*ahpF2*)	61.9
A1S_1200	Alkyl hydroperoxide reductase subunit F (*ahpF1*)	49.3
A1S_1458	Alkyl hydroperoxide reductase subunit F (*ahpF2*)	47.2
A1S_1201	Alkyl hydroperoxide reductase subunit F (*ahpF1*)	40.3
A1S_1460	Alkyl hydroperoxide reductase subunit F (*ahpF2*)	35.7
A1S_3382	Catalase (*katE*)	27.7
A1S_2863	Putative antioxidant protein	5.9
Sulfur homeostasis		
A1S_2533	Putative esterase	459.7
A1S_2532	Sulfate transport protein	364.5
A1S_2531	Sulfate transport system substrate-binding protein	334.4
A1S_2534	Sulfate transport system permease protein	172.9
A1S_0030	Sulfonate transport system substrate-binding protein	165.8
A1S_0028	Alkanesulfonate monooxygenase	113.7
A1S_2535	Sulfate transport system permease protein	106.1
A1S_0029	Sulfonate transport system substrate-binding protein	71.2
A1S_0027	Sulfonate transport system permease protein	49.6
A1S_3207	Sulfate transport system substrate-binding protein	46.0
A1S_1408	Putative rhodanese-related sulfurtransferase	25.5
A1S_2536	Sulfate transport system ATP-binding protein	18.1
A1S_0977	Arylsulfatase	18.0
A1S_3306	Dimethylsulfone monooxygenase	17.9
A1S_0026	Sulfonate transport system ATP-binding protein	16.2
A1S_2846	Sulfite reductase (NADPH) hemoprotein beta-component	5.6
Iron homeostasis		
A1S_2389	Iron complex transport system permease protein	26.2
A1S_2381	2,3-Dihydroxybenzoate-AMP ligase	21.8
A1S_1719	4Fe-4S ferredoxin iron-sulfur binding	21.4
A1S_2380	Bifunctional isochorismate lyase	18.2
A1S_2379	Histidine decarboxylase	16.3
A1S_2382	BasD	16.0
A1S_2388	Iron complex transport system permease protein	15.8
A1S_2387	Iron complex transport system ATP-binding protein	14.9
A1S_2390	Putative acinetobactin biosynthesis protein	8.7
A1S_2372	Isochorismate synthase	8.2
A1S_2386	Iron complex transport system substrate-binding protein	7.4
A1S_2383	Putative acinetobactin biosynthesis protein	6.9
A1S_2392	Putative acinetobactin utilization protein	6.1
A1S_2077	Putative outer membrane porin receptor for Fe(III)-coprogen, Fe(III)-ferrioxamine B, and Fe(III)-rhodotorulic acid uptake (*fhuE*)	5.7
A1S_3339	Iron complex outer membrane receptor protein	5.4
A1S_1607	Iron complex outer membrane receptor protein	4.6
A1S_1647	Putative siderophore biosynthesis protein	4.4
A1S_1359	Iron(III) transport system substrate-binding protein	4.3
A1S_2530	4-Amino-4-deoxychorismate lyase	4.1
A1S_1634	Rrf2 family transcriptional regulator	4.1
Phosphate transport		
A1S_2448	Phosphate transport system substrate-binding protein	10.5
A1S_2447	Phosphate transport system permease protein	6.8
A1S_3374	Positive Pho regulon response regulator	6.0
A1S_3376	Phosphate regulon sensor histidine kinase PhoR	4.7
A1S_0256	Phosphate transport system protein	4.4
Nucleic acid synthesis and repair		
A1S_2273	RNA 3′-terminal phosphate cyclase (ATP)	26.4
A1S_2586	dGTP triphosphohydrolase	8.6
A1S_0310	Excinuclease ABC subunit C	6.4

(Continued on next page)

TABLE 1 (Continued)

Category and locus	Annotation (KEGG)[a]	Fold change
A1S_1173	DNA polymerase V	5.3
A1S_2008	DNA polymerase V	4.8
A1S_0636	DNA polymerase V	4.8
A1S_1174	DNA polymerase V	4.6
A1S_1962	Recombination protein RecA	4.4
A1S_3295	Excinuclease ABC subunit A	4.2
A1S_3359	Topoisomerase IV subunit B	4.1
Amino acid transport and metabolism		
A1S_1443	Taurine transport system ATP-binding protein	222.8
A1S_0023	Putative malic acid transport protein	135.0
A1S_1397	Polar amino acid transport system permease protein	102.2
A1S_1444	Taurine transport system permease protein	87.3
A1S_1442	Taurine transport system substrate-binding protein	85.9
A1S_1396	Polar amino acid transport system permease protein	76.5
A1S_1445	Taurine dioxygenase	41.8
A1S_1398	Polar amino acid transport system ATP-binding protein	27.1
A1S_0921	Arginine:ornithine antiporter/lysine permease	14.7
A1S_1399	Polar amino acid transport system substrate-binding protein	11.4
A1S_1485	D-Methionine transport system substrate-binding protein	9.9
A1S_2384	Lysine N^6-hydroxylase	6.6
A1S_1046	Lysine exporter	6.3
A1S_1407	Serine *O*-acetyltransferase	6.1
A1S_1400	Polar amino acid transport system substrate-binding protein	4.8
Ribosome		
A1S_2271	tRNA-splicing ligase RtcB	118.6
A1S_1961	Ribosome-associated heat shock protein Hsp15	5.1
Fatty acid metabolism		
A1S_1436	Putative acyl-CoA dehydrogenase	7.8
A1S_1437	Putative acyl-CoA dehydrogenase	7.7
A1S_2458	Linoleoyl-CoA desaturase	7.5
A1S_0394	Putative acyl-CoA dehydrogenase	7.4
Transport		
A1S_1456	Chromate transporter	23.1
A1S_1457	Chromate transporter	13.1
A1S_2378	Putative ABC transporter	8.4
A1S_1720	NitT/TauT family transport system substrate-binding protein	8.2
A1S_3272	MFS transporter, YNFM family, putative membrane transport protein	5.7
A1S_2377	Putative ABC transporter	5.4
A1S_2311	ABC-2 type transport system ATP-binding protein	4.4
A1S_1772	MFS transporter, DHA2 family, multidrug resistance protein	4.2
Metabolism (other)		
A1S_1488	Putative acyl-CoA dehydrogenase	100.9
A1S_1487	Putative acyl-CoA dehydrogenase	30.0
A1S_3305	FMN reductase	24.6
A1S_1486	Putative monooxygenase (DszA-like)	24.5
A1S_0922	Putative homocysteine *S*-methyltransferase family protein	19.9
A1S_0393	Putative acyl-CoA dehydrogenase	15.3
A1S_0024	Adenosylhomocysteine nucleosidase	10.9
A1S_0463	Putative alkaline phosphatase	9.0
A1S_2459	Putative oxidoreductase	8.3
A1S_3222	Homocysteine synthase	6.9
A1S_2293	Ferredoxin/flavodoxin–$NADP^+$ reductase	5.5
A1S_1446	Allantoin racemase	4.4
A1S_0131	Streptomycin 3″-adenylyltransferase	4.3
Other		
A1S_1717	GntR family transcriptional regulator	32.1

(Continued on next page)

TABLE 1 (Continued)

Category and locus	Annotation (KEGG)[a]	Fold change
A1S_1414	LrgB-like protein	27.5
A1S_0466	Sec-independent protein translocase protein TatA	25.0
A1S_1665	Putative membrane protein	19.9
A1S_3114	CBS domain-containing membrane protein	19.0
A1S_1677	Putative porin precursor	17.5
A1S_3381	AnkB protein	17.4
A1S_0465	Sec-independent protein translocase protein TatB	16.1
A1S_1963	Regulatory protein	13.2
A1S_0464	Sec-independent translocation protein TatC	12.8
A1S_1928	Putative signal peptide	12.4
A1S_2473	Transcriptional regulator, LysR family	10.4
A1S_1224	Transposase	8.9
A1S_0416	Putative transcriptional regulator (LysR family)	5.9
A1S_3326	Putative membrane protein	5.4
A1S_1438	Putative coenzyme F_{420}-dependent N^5,N^{10}-methylene tetrahydromethanopterin reductase	5.2
A1S_3375	Phosphate regulon response regulator PhoB	5.2
A1S_1539	ArsR family transcriptional regulator	4.7
A1S_1767	Putative acid phosphatase	4.7
A1S_1503	Transmembrane pair	4.5
A1S_3360	Putative esterase	4.3
A1S_2319	Putative membrane protein	4.2
A1S_0565	Putative membrane protein	4.2
A1S_1197	Putative extracellular nuclease	4.1
Hypothetical		
A1S_0517	Hypothetical protein	139.3
A1S_3813	Hypothetical protein	73.1
A1S_3666	Hypothetical protein	47.7
A1S_3906	Hypothetical protein	43.9
A1S_1718	Hypothetical protein	30.1
A1S_2272	Hypothetical protein	26.2
A1S_3783	Hypothetical protein	21.5
A1S_3116	Hypothetical protein	15.4
A1S_3115	Hypothetical protein	14.6
A1S_3668	Hypothetical protein	13.6
A1S_3804	Hypothetical protein	12.5
A1S_0617	Hypothetical protein	12.2
A1S_3782	Hypothetical protein	9.5
A1S_3913	Hypothetical protein	8.1
A1S_0889	Hypothetical protein	8.0
A1S_1390	Hypothetical protein	7.7
A1S_0976	Hypothetical protein	7.0
A1S_2266	Hypothetical protein	6.9
A1S_3113	Hypothetical protein	5.9
A1S_0224	Hypothetical protein	5.6
A1S_1614	Hypothetical protein	5.5
A1S_3878	Hypothetical protein	5.5
A1S_3479	Hypothetical protein	5.2
A1S_3780	Hypothetical protein	5.1
A1S_3682	Hypothetical protein	5.1
A1S_2267	Hypothetical protein	4.9
A1S_3912	Hypothetical protein	4.9
A1S_3638	Hypothetical protein	4.7
A1S_3849	Hypothetical protein	4.1
A1S_0770	Hypothetical protein	4.1
A1S_3513	Hypothetical protein	4.1

[a]CoA, coenzyme A; MFS, major facilitator superfamily; CBS, cystathionine β-synthase; FMN, flavin mononucleotide.

droperoxide reductase (19, 26, 37). Since *A. baumannii* is known to encode an OxyR homologue (33), we hypothesized that OxyR is important for the transcriptional changes induced by H_2O_2. To test this hypothesis, an *A. baumannii* mutant (Δ*oxyR*) that contained an in-frame replacement of *oxyR* (*A1S_0992*) with the kanamycin resistance cassette *aph1* was generated. The transcriptional profile of the Δ*oxyR* strain in the

TABLE 2 Genes with increased expression in the Δ*oxyR* strain following treatment with H_2O_2

Category and locus	Annotation	Fold change
Nucleic acid synthesis and repair		
A1S_2008	DNA polymerase V	4.9
A1S_1389	DNA polymerase V	4.2
Transport		
A1S_3272	MFS transporter, YNFM family, putative membrane transport protein	7.8
Metabolism (other)		
A1S_0567	NAD(P) transhydrogenase subunit alpha	12.4
A1S_0566	NAD(P) transhydrogenase subunit alpha	11.3
A1S_0568	NAD(P) transhydrogenase subunit beta	9.8
Hypothetical		
A1S_3510	Hypothetical protein	9.8
A1S_0617	Hypothetical protein	9.4
A1S_3704	Hypothetical protein	7.8
A1S_1151	Hypothetical protein	7.0
A1S_3705	Hypothetical protein	5.0
A1S_3116	Hypothetical protein	4.5
A1S_3115	Hypothetical protein	4.5
A1S_1150	Hypothetical protein	4.4

presence and absence of H_2O_2 was characterized by RNA sequencing (Fig. 2B; Table 2; see also Table S3 in the supplemental material). In accord with our hypothesis, only 15 genes were upregulated by H_2O_2 in the Δ*oxyR* mutant, demonstrating that *oxyR* is important for activating the transcriptional response to H_2O_2. To validate the RNA-sequencing results, reverse transcription-quantitative PCR (qRT-PCR) was performed to measure the transcript abundance of selected genes that exhibited the most significant changes in expression in the transcriptome sequencing (RNA-seq) data (Fig. 2C). The abundances of the *A1S_1200* (*ahpF1*), *A1S_1458* (*ahpF2*), *A1S_2459* (oxidoreductase), and *A1S_2531* (sulfate transporter) transcripts were significantly increased following H_2O_2 treatment in an *oxyR*-dependent manner, while the abundances of the *A1S_0104* (acyl coenzyme A [acyl-CoA] synthesis) and *A1S_2150* (oxidoreductase) transcripts were significantly decreased in an *oxyR*-dependent manner. Together, these results demonstrate that in *A. baumannii*, OxyR is an important global regulator of the transcriptional response to H_2O_2.

Inactivation of *oxyR* impairs *A. baumannii* growth in the presence of H_2O_2. Based on the inability of the Δ*oxyR* strain to upregulate detoxification genes upon exposure to H_2O_2, we hypothesized that the Δ*oxyR* strain would have a growth deficiency in a medium containing H_2O_2. The *A. baumannii* Δ*oxyR* strain did not have a significant growth defect in lysogeny broth (LB) and, in fact, grew to a higher cell density than the wild type (WT) in stationary phase (see Fig. S1A in the supplemental material). However, when the strains were grown in the presence of 100 μM H_2O_2, the lag time for the Δ*oxyR* strain was 6 h longer than that for the WT (Fig. 3A). The growth lag of the Δ*oxyR* strain in H_2O_2 was complemented by expressing *oxyR* in *trans* under the control of a constitutive promoter (Fig. S1B in the supplemental material). The growth of the Δ*oxyR* strain was impaired by concentrations of H_2O_2 as low as 50 μM (Fig. 3B). Similarly, in a H_2O_2 disc diffusion assay, the Δ*oxyR* strain exhibited a substantially greater zone of inhibition by H_2O_2 than the WT (Fig. 3C and D).

A gene encoding OxyR is present in every annotated *A. baumannii* genome, suggesting that its regulatory role is conserved within the species (see Table S4 in the supplemental material). We evaluated the role of *oxyR* in the growth of the *A. baumannii* strain AB5075, a multidrug-resistant clinical isolate. AB5075 mutant strains with transposons (Tn) within the *oxyR* allele (*ABUW_2905*) were obtained from the University of Washington sequenced-

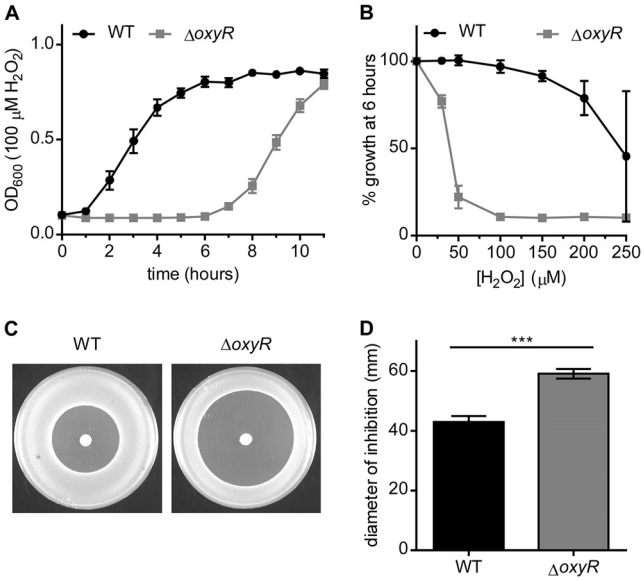

FIG 3 Inactivation of *oxyR* impairs the growth of *A. baumannii* in the presence of H_2O_2. (A to D) The growth of WT *A. baumannii* and the Δ*oxyR* strain was monitored under various conditions. (A) The growth of *A. baumannii* in LB containing 100 μM H_2O_2 was monitored by the OD_{600}. (B) Inhibition of growth by H_2O_2 at the concentrations indicated on the *x* axis at the 6-h time point. Growth as a percentage of the growth of the corresponding untreated strain. For panels A and B, growth curves are from a single experiment performed in biological triplicate and are representative of the results of three independent experiments. (C) Zone of inhibition by 10 μl of 9.8 M H_2O_2 spotted onto discs placed on solid medium. Representative plates are shown after overnight growth. (D) Quantification of the diameter of inhibition by H_2O_2. Data are combined from three independent experiments with three biological replicates in each experiment. Triple asterisks (***) indicate a *P* value of <0.001 by Student's *t* test.

transposon library (38). Four independent *ABUW_2905*::Tn mutants were evaluated for growth in LB in the absence or presence of H_2O_2. In contrast to the 17978 *oxyR* mutant, AB5075 *ABUW_2905*::Tn mutants exhibited impaired growth in LB (Fig. S1C in the supplemental material). Decreased growth in the absence of exogenous H_2O_2 has been observed previously for *oxyR* mutants in other organisms (39). In the presence of H_2O_2, *ABUW_2905*::Tn mutants show striking growth impairment (Fig. S1D and E in the supplemental material). Taken together, these results demonstrate that *oxyR* is important for the growth of multiple *A. baumannii* strains in the presence of H_2O_2.

A conserved cysteine residue is important for OxyR function. A phylogenetic analysis comparing *A. baumannii* OxyR to other characterized OxyR proteins revealed that *A. baumannii* OxyR is in the same clade as OxyR from other *Proteobacteria* (Fig. 4A). In *E. coli*, OxyR senses H_2O_2 by a hyperreactive thiol in a conserved cysteine residue (C199) that is rapidly oxidized by H_2O_2 (37). Mutational analysis of *E. coli* demonstrated that mutation of this cysteine residue to serine locks OxyR in the reduced state (40). Alignment of the primary amino acid sequence revealed that C202 in *A. baumannii* OxyR aligns with C199 in *E. coli* (Fig. 4B). Therefore, we hypothesized that C202 is important for the function of *A. baumannii* OxyR. Expression of *oxyR* with cysteine 202 mutated to serine in *trans* did not complement the growth defect of the Δ*oxyR* strain in H_2O_2 (Fig. 4C). These data suggest that this conserved cysteine residue is critical for the function of OxyR in *A. baumannii*.

***A. baumannii* Δ*oxyR* is preadapted to H_2O_2 stress.** We next investigated whether OxyR altered the survival of *A. baumannii* cultures in a H_2O_2 killing assay. As expected, increasing concentrations of H_2O_2 resulted in decreased survival of WT *A. baumannii* (Fig. 5A). However, the Δ*oxyR* strain was resistant to killing by H_2O_2 under these conditions, with no decrease in survival until 40 mM H_2O_2 was applied (Fig. 5A). Based on these results, we hypothesized that the Δ*oxyR* strain is protected from H_2O_2 killing because this strain has altered expression of the peroxide detoxification machinery in

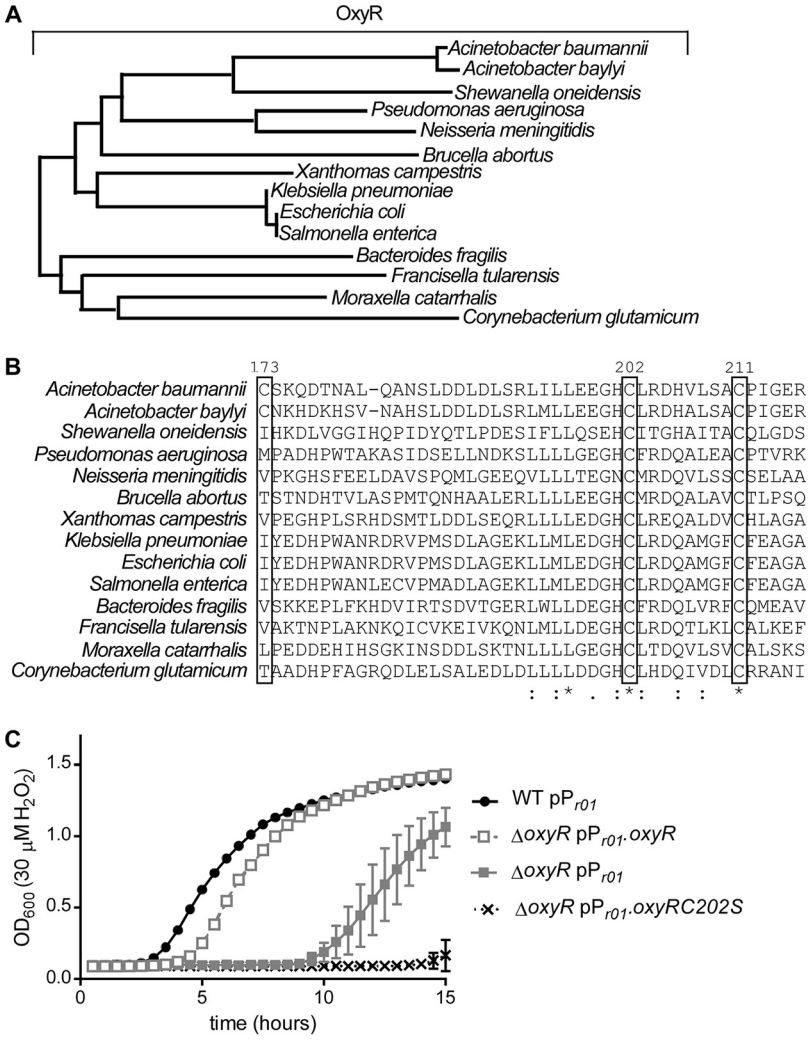

FIG 4 *A. baumannii* OxyR contains a conserved cysteine residue that is important for function. (A) Phylogenetic tree based on protein sequence alignment of *A. baumannii* and *Acinetobacter baylyi* OxyR with experimentally characterized OxyR proteins in other Gram-negative organisms. Branch lengths are representative of sequence divergence. (B) Amino acid sequence alignment for a portion of the substrate-binding domain of OxyR that contains conserved cysteine residues. An asterisk indicates complete conservation; one dot indicates similar residues at a particular position; and two dots indicate highly similar residues at a particular position. Boxed amino acid positions contain a cysteine in the *A. baumannii* OxyR sequence. (C) Growth of WT *A. baumannii* with an empty vector, the Δ*oxyR* strain with an empty vector, the Δ*oxyR* strain expressing WT *oxyR* in *trans,* or the Δ*oxyR* strain expressing *oxyR C202S* in *trans* in 30 μM H_2O_2. The growth curves are from a single experiment performed in biological triplicate and are representative of the results of three independent experiments.

LB. To test this hypothesis, the RNA-seq data were analyzed to compare the transcriptional profiles of WT *A. baumannii* and the Δ*oxyR* strain in LB (Table 3; see also Table S5 in the supplemental material). In results consistent with our model, the Δ*oxyR* strain expressed higher levels of *ahpF1* (*A1S_1200–1201*), *ahpF2* (*A1S_1458–1460*), and *katE* (*A1S_3382*) in LB, and these findings were confirmed by qRT-PCR (Fig. 5B). Because these genes are also induced by H_2O_2 exposure, we posited that low-dose H_2O_2 exposure adapts *A. baumannii* to H_2O_2 stress, protecting against killing by higher concentrations of H_2O_2. Indeed, pretreatment with 1 mM H_2O_2 enhanced the survival of WT *A. baumannii* following high-dose H_2O_2 stress (Fig. 5C). However, pretreatment of the Δ*oxyR* strain with 1 mM H_2O_2 did not alter the survival of this strain, suggesting that the Δ*oxyR* strain is preadapted to H_2O_2 stress (Fig. 5C). Together, these results reveal that *A. baumannii* adapts to H_2O_2 stress and that the Δ*oxyR* strain is phenotypically preadapted to H_2O_2 stress and resistant to H_2O_2 killing. This result is consistent

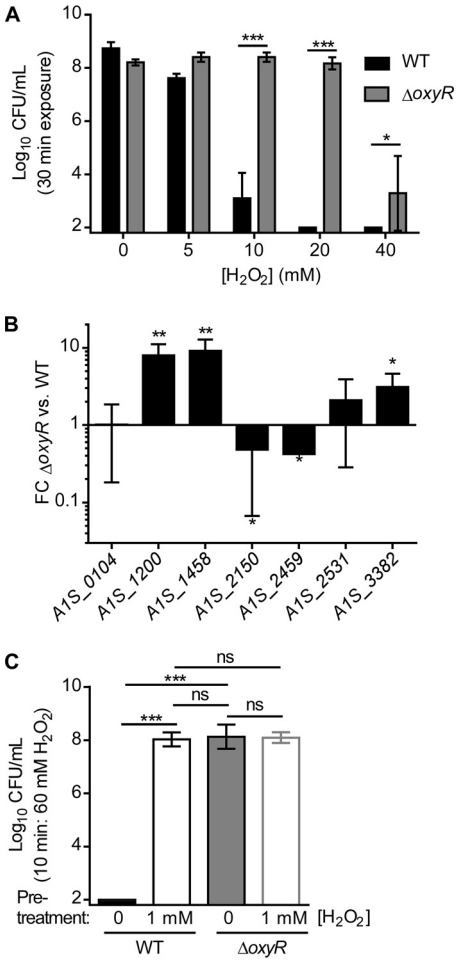

FIG 5 *A. baumannii* with *oxyR* inactivated is preadapted to H_2O_2 stress during exponential growth. (A) Mid-exponential-phase cultures of WT *A. baumannii* and the Δ*oxyR* strain were treated with bolus doses of H_2O_2 at the indicated concentrations for 30 min. CFU enumerated following bolus exposure are shown on a $\log_{10}$ scale. The limit of detection was 2 $\log_{10}$ CFU. Asterisks indicate significant differences (*, $P < 0.05$; ***, $P < 0.001$) by *t* test. Bars indicate means ± standard deviations. (B) qRT-PCR quantification of the relative abundances of H_2O_2-responsive transcripts in WT *A. baumannii* and the Δ*oxyR* strain in LB alone. FC, fold change. Asterisks indicate significant differences (*, $P < 0.05$; **, $P < 0.01$) by *t* test against a theoretical value of 1.0. Six biological replicates were run. Results are means ± standard deviations. For panels A and B, data are from a single experiment performed in biological triplicate and are representative of five independent experiments. (C) Mid-exponential-phase cultures of the *A. baumannii* WT and Δ*oxyR* strains were pretreated with 1 mM H_2O_2 or a vehicle for 30 min. Following pretreatment, cultures were exposed to a bolus of 60 mM H_2O_2 for 10 min. CFU enumerated following bolus exposure are shown on a $\log_{10}$ scale with the limit of detection at 2 $\log_{10}$ CFU. Asterisks indicate significant differences (*, $P < 0.05$; ***, $P < 0.001$) by one-way analysis of variance with Tukey's multiple-comparison test. ns, no significant difference. Bars indicate means ± standard deviations.

with the finding that *ahpF1* (*A1S_1200–1201*), *ahpF2* (*A1S_1458–1460*), and *katE* (*A1S_3382*) expression does not increase with H_2O_2 treatment in the Δ*oxyR* strain (Fig. 2C) but that expression is high in the absence of H_2O_2 (Fig. 5B). Mechanistically, these data suggest that OxyR functions as a repressor of the *ahpF1* (*A1S_1200–1201*), *ahpF2* (*A1S_1458–1460*), and *katE* (*A1S_3382*) genes, since the Δ*oxyR* strain overexpresses these genes.

OxyR binds to the promoters of *ahp* and *kat*. We hypothesized that OxyR directly binds to the promoter regions of genes encoding H_2O_2 detoxification machinery. To determine if OxyR directly binds the promoter regions of putative target genes in a H_2O_2-dependent manner, electromobility shift assays (EMSAs) were carried out with OxyR bearing an N-terminal hexahistidine tag (see Fig. S2A in the supplemental material). OxyR was purified under reducing conditions, and promoter binding was

TABLE 3 Genes with increased expression in the Δ*oxyR* strain in LB

Category and locus	Annotation (KEGG)	Fold change
Peroxide detoxification		
A1S_1458	Alkyl hydroperoxide reductase subunit F (*ahpF2*)	8.4
A1S_1200	Alkyl hydroperoxide reductase subunit F (*ahpF1*)	8.3
A1S_1201	Alkyl hydroperoxide reductase subunit F (*ahpF1*)	7.9
A1S_1459	Alkyl hydroperoxide reductase subunit F (*ahpF2*)	7.4
A1S_1460	Alkyl hydroperoxide reductase subunit F (*ahpF2*)	7.3
A1S_1458	Alkyl hydroperoxide reductase subunit F (*ahpF2*)	8.4
Sulfur homeostasis		
A1S_2531	Sulfate transport system substrate-binding protein	4.6
A1S_2533	Putative esterase	4.5
Iron homeostasis		
A1S_1647	Putative siderophore biosynthesis protein	4.4
Amino acid transport and metabolism		
A1S_1528	Hypothetical	24.0
A1S_3046	Oligopeptidase A	5.2
A1S_3047	Oligopeptidase A	5.1
Chaperones		
A1S_2959	Molecular chaperone GrpE	5.1
A1S_2960	Molecular chaperone DnaK	4.6
A1S_2665	K04078 chaperonin GroES	4.4
Metabolism (other)		
A1S_0804	Trehalose 6-phosphate phosphatase	4.6
Other		
A1S_0646	Intracellular multiplication protein IcmB	4.5
A1S_0647	Intracellular multiplication protein IcmO	4.5
Hypothetical		
A1S_3873	Hypothetical protein	19.0
A1S_3546	Hypothetical protein	4.9

tested in the presence or absence of excess H_2O_2. OxyR binds the promoter regions of *A1S_1201* (*ahpF1*) and *A1S_3382* (*katE*), and binding occurs with lower concentrations of OxyR following incubation with H_2O_2 (Fig. 6A and B). To test the hypothesis that the cysteine at position 202 is important for the regulation of DNA binding activity, the binding of recombinant OxyR C202S to the promoter region of *A1S_1201* (*ahpF1*) was assessed. In the presence of H_2O_2, a DNA mobility shift was present at lower concentrations of protein for WT OxyR than for OxyR C202S, suggesting that under these conditions, C202 is important for DNA binding activity (Fig. 6C). Interestingly, under reducing conditions, OxyR C202S had DNA binding activity similar to that of WT OxyR, suggesting that C202 is not important for DNA binding activity in the absence of H_2O_2 (Fig. 6D). In addition, OxyR C202S was capable of binding the promoter region of *A1S_3382* (*katE*) similarly to WT OxyR under reducing conditions but demonstrated decreased binding in the presence of H_2O_2 (Fig. S2B in the supplemental material). WT OxyR and OxyR C202S did not cause DNA shifts of the negative-control *mumT* promoter (Fig. S2C in the supplemental material). Together, these data demonstrate that *A. baumannii* OxyR is a DNA-binding protein that exhibits differential DNA binding ability for target genes following exposure to H_2O_2. Furthermore, C202 modulates binding to target DNA promoters in the presence of H_2O_2 but not in the absence of H_2O_2. The fact that OxyR binds to the promoter regions of *ahpF1* and *katE* in the absence of H_2O_2 is consistent with the model that *A. baumannii* OxyR is a repressor of these genes in the absence of H_2O_2.

***oxyR* promotes the fitness of *A. baumannii* in a murine model of pneumonia.** Since H_2O_2 is produced in the lung during *A. baumannii* pneumonia and OxyR orches-

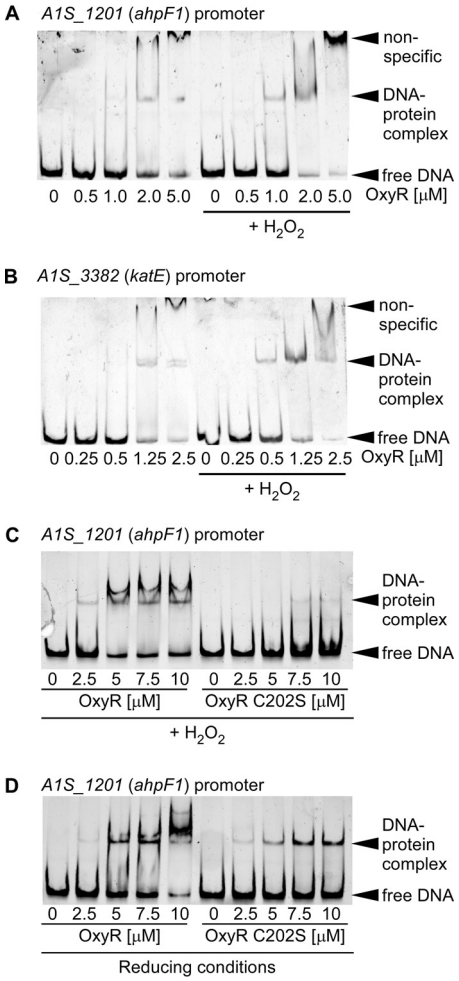

FIG 6 OxyR binds the promoters of *ahp* and *kat*. (A to D) PCR-amplified promoter regions for *A1S_1201* (*ahpF1*) (A, C, and D) or *A1S_3382* (*katE*) (B) were incubated with purified recombinant His_6-OxyR alone (A and B) or with WT His_6-OxyR or His_6-OxyR C202S (C and D). The protein was preincubated for 10 min with or without 50 mM H_2O_2. DNA was visualized using SYBR green. Each gel is representative of experiments performed on at least two separate days.

trates the transcriptional response to H_2O_2 *in vitro*, we hypothesized that OxyR promotes the fitness of *A. baumannii* during infection of the murine lung. Mice were coinfected intranasally with WT *A. baumannii* and the Δ*oxyR* strain, and bacterial burdens were enumerated 36 h postinfection. The Δ*oxyR* strain was recovered at significantly lower numbers than WT *A. baumannii* in the lung (Fig. 7A), indicating that the WT is more fit than the Δ*oxyR* strain. The Δ*oxyR* strain was also less able to disseminate to the liver (Fig. 7B). Therefore, *oxyR* promotes the fitness of *A. baumannii* during infection.

DISCUSSION

We report here that *A. baumannii* encounters H_2O_2 during infection of the murine lung and employs a sophisticated strategy to survive and grow in the presence of H_2O_2. Transcriptional profiling of *A. baumannii* exposed to H_2O_2 revealed that the canonical *oxyR* regulon is induced by H_2O_2 in an *oxyR*-dependent manner. *A. baumannii* lacking *oxyR* has impaired growth in the presence of H_2O_2, but the Δ*oxyR* strain overexpresses *ahp* and *katE* during aerobic growth and is protected from H_2O_2-mediated killing. We demonstrate that *A. baumannii* OxyR contains a functionally important conserved cysteine residue and exhibits H_2O_2-dependent promoter binding activity. Finally, *oxyR* confers a fitness advantage in a competitive murine model of pneumonia.

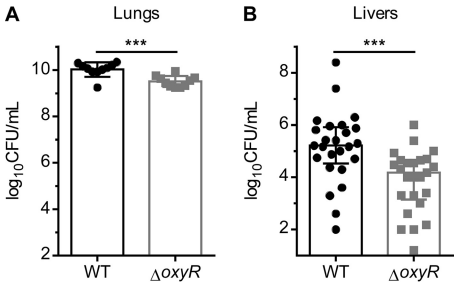

FIG 7 *oxyR* promotes the fitness of *A. baumannii* in a murine model of pneumonia. (A and B) Bacterial burdens were enumerated from the lungs (A) and livers (B) of mice 36 h following intranasal inoculation of a 1:1 mixture of WT *A. baumannii* or the Δ*oxyR* strain. (A) Lung CFU. Data are from one experiment ($n = 10$). (B) Liver CFU. Data are combined from two independent experiments ($n = 25$). Triple asterisks (***) indicate a P value of <0.001 by the Mann-Whitney test.

People who lack an effective neutrophil oxidative burst due to mutations in NADPH oxidase develop frequent and severe infections due to catalase-producing organisms, emphasizing the importance of the neutrophil oxidative burst in protection against infection (41). While the production of H_2O_2 by neutrophils can be monitored easily in cell culture assays (42), visualization of the neutrophil oxidative burst that occurs during infection presents a technical challenge, because reactive oxygen and nitrogen species are, by definition, highly reactive. Here we used a recently described chemical probe to detect *in vivo* H_2O_2 production in real time in a live animal. We found that infection of the lung with *A. baumannii* instigated H_2O_2 production specifically within the thoracic cavity, illustrating the harsh environment that *A. baumannii* must endure in order to successfully colonize the lung and cause disease.

RNA sequencing of *A. baumannii* exposed to H_2O_2 revealed a robust transcriptional response that shared some transcriptional changes with the findings of previously published RNA-sequencing and microarray experiments in other bacteria (27, 43–53). Interestingly, RNA sequencing revealed that H_2O_2 exposure leads to the downregulation of many metabolic genes, including the *paa* operon, which has been shown to enhance the virulence of *A. baumannii* in a murine sepsis model and a zebrafish infection model (54, 55). Analysis of the RNA-sequencing data provides insight into genes that may be activated by OxyR in the presence of H_2O_2. Compared to the well-studied OxyR regulon in *E. coli* (21), *A. baumannii* shares upregulation of *ahpF1*, *ahpF2*, and catalase, but not other genes known to be regulated by *E. coli* OxyR, including *fur*, *hemH*, *trxB*, *trxC*, *gorA*, or *grxA*. Thus, while OxyR is highly conserved among Gram-negative bacteria, the OxyR regulon is not conserved across the *Gammaproteobacteria*, highlighting the functional diversity of this regulator.

A. baumannii Δ*oxyR* shares characteristics with *oxyR* mutants in multiple organisms. Inactivation of *oxyR* in *A. baumannii* increases the zone of inhibition by H_2O_2 in a disc diffusion assay, a finding similar to those for *B. abortus*, *Pseudomonas aeruginosa*, *Moraxella catarrhalis*, and *E. coli* (28, 48, 53, 56). Elucidating the contribution of *oxyR* to H_2O_2 stress resistance adds to existing knowledge of genes that protect against H_2O_2 toxicity in *A. baumannii*, including *uspA*, *katE*, and *katG* (16, 17).

In addition to its role in coordinating the response to exogenous H_2O_2, OxyR may also be important in the context of endogenous H_2O_2. Indeed, in *A. baumannii* strain AB5075, inactivation of *oxyR* leads to a decreased growth rate in the absence of exogenously added H_2O_2. In contrast, inactivation of *oxyR* in *A. baumannii* strain ATCC 17978 leads to higher optical density (OD) of stationary-phase cultures. One potential explanation for the finding that *oxyR* mutants have growth phenotypes in the absence of exogenous H_2O_2 is that *A. baumannii* OxyR may be important for protecting against endogenously produced H_2O_2, as has been shown in *E. coli*, where OxyR induces H_2O_2-scavenging enzymes in response to phenylethylamine oxidase-generated H_2O_2 (57). However, another possible explanation of these data is that OxyR plays a role in fundamental cellular metabolism. Loss of *oxyR* reduces the efficacy of oxygen respira-

tion in *Shewanella oneidensis* and increases the transcription of cytochrome *bd* (39); while no significant differences in *cyd* operon expression were noted in the RNA sequencing of the *A. baumannii* Δ*oxyR* strain in LB, it is possible that other aspects of central metabolism are altered in this strain. Much remains to be learned about the function of OxyR in pathogenic organisms, including its potential role in central metabolism. For instance, all *Mycobacterium tuberculosis* isolates carry inactivated *oxyR* alleles (58), suggesting that *oxyR* may be detrimental in some infectious niches and that the biological role of this protein remains incompletely understood. Exploring central metabolism using *oxyR*-null strains may provide insight into this biology.

Like *B. abortus* and *N. meningitidis* (28, 30), the *A. baumannii* Δ*oxyR* strain is resistant to H_2O_2 in exponential phase. This resistance correlates with the increased transcription of *katE*, *ahpF1*, and *ahpF2* in the Δ*oxyR* strain in the absence of H_2O_2. There are at least two possible models to explain the upregulation of *ahpF1*, *ahpF2*, and *katE* in the *oxyR* mutant. The first model is that loss of *oxyR* induces the upregulation of *oxyR*-independent pathways that lead to increased transcription of hydrogen peroxide detoxification genes. The second model is that OxyR has a dual function as both a repressor and an activator of *ahpF1*, *ahpF2*, and *katE* depending on the oxidation state of OxyR, which has been proposed previously for OxyR in other organisms, including *N. meningitidis* and *S. oneidensis* (30, 59). In this dual repressor-activator model, reduced OxyR binding to the promoter represses transcription and oxidized OxyR binding to the promoter activates transcription. Based on this hypothesis, loss of *oxyR* would lead to derepression of *ahpF1*, *ahpF2*, and *katE* in the absence of hydrogen peroxide and thus to an increase in the basal level of transcription. We propose that the *A. baumannii* Δ*oxyR* strain is resistant to H_2O_2 killing because of the higher transcription of *katE*, *ahpF1*, and *ahpF2* in the absence of H_2O_2, and increased transcription of the detoxification machinery provides resistance to bolus dosing of H_2O_2. It would be interesting to test the hypothesis that the increased resistance to H_2O_2 in the *oxyR* deletion strain is due to upregulation of *ahpF1*, *ahpF2*, and *katE* through the generation of double, triple, or quadruple mutant strains, although this undertaking would be technically challenging, and analysis of the combination mutants would not be straightforward, since each mutant is likely to have a phenotype independently. Taken together, these results highlight the importance of OxyR as a transcriptional regulator in both reduced and oxidative environments.

This work provides evidence that *A. baumannii* OxyR functions as both a transcriptional repressor and a transcriptional activator. H_2O_2 induces expression of OxyR gene targets, including *ahpF1* and *katE*, in an OxyR-dependent manner. This result suggests that OxyR is an activator. However, *ahpF1* and *katE* have higher expression in the Δ*oxyR* strain in the absence of exogenous H_2O_2, in accord with repression by OxyR at these promoters. OxyR binds the *ahpF1* and *katE* promoter regions with greater affinity following incubation with H_2O_2, in accord with a mechanism of OxyR activation by oxidation of C202, but binding is not abolished in the absence of H_2O_2. The finding that OxyR C202S is capable of binding the promoters of *ahpF1* and *katE* under reducing conditions, but binds less well under oxidizing conditions, is consistent with the model that this residue is important for regulating DNA binding in the presence of H_2O_2. Therefore, we propose that OxyR binds to these promoters in the absence of a signal and represses transcription. Following activation by H_2O_2, OxyR undergoes a conformational change and activates transcription of the target genes. This dual repressor/activator function has been described previously for regulation of the *ahpC* promoter by OxyR in *X. campestris* (60). However, another possible explanation for increased expression of *ahpF1*, *ahpF2*, and *katE* in the absence of *oxyR* is that another transcriptional regulator can be activated by endogenous peroxide when OxyR is absent.

Previous studies with *E. coli* have demonstrated that sensing of H_2O_2 requires a conserved cysteine residue at position 199. Oxidation of C199 results in a significant structural change to the regulatory domain of *E. coli* OxyR (22). In this work, we demonstrate that C202 is important for the function of *A. baumannii* OxyR. Interestingly, the *oxyR* deletion strain complemented with *oxyR C202S* grows more poorly in

TABLE 4 Bacterial strains used in this study

Strain	Relevant characteristics	Reference or source
Acinetobacter baumannii 17978	Wild-type *Acinetobacter baumannii*	ATCC
Acinetobacter baumannii 17978 Δ*oxyR*	In-frame Δ*oxyR*::*aphA*	This study
Acinetobacter baumannii 17978 pWH1266	Empty-vector control with plasmid pP_{r01}WH1266	78
Acinetobacter baumannii 17978 Δ*oxyR* pWH1266	Empty-vector control with plasmid pP_{r01}WH1266	This study
Acinetobacter baumannii 17978 Δ*oxyR* p*oxyR*WH1266	Complementation strain containing plasmid p.P_{r01}.*oxyR*.WH1266	This study
Acinetobacter baumannii 17978 Δ*oxyR* p*oxyR* C202S WH1266	Complementation strain containing plasmid p.P_{r01}.*oxyR*.WH1266 with C202S mutation	This study
Acinetobacter baumannii 17978 pAT02	Wild type harboring rec_{Ab} machinery for recombineering	33
Escherichia coli DH5α p.*oxyR*	Cloning strain containing plasmid p.P_{r01}.*oxyR*.WH1266	This study
Escherichia coli DH5α p.*oxyR* C202S	Cloning strain containing plasmid p.P_{r01}.*oxyR*.WH1266 with C202S mutation	This study
Escherichia coli DH5α p.*oxyR* pCRBlunt	Cloning strain containing *oxyR* in pCR-Blunt	This study
Escherichia coli DH5α p.*oxyR* C202S pCRBlunt	Cloning strain containing *oxyR* with C202S mutation in pCR-Blunt	This study
Escherichia coli BL21(DE3) p.*oxyR*.ET15B	Protein expressing strain for *oxyR* cloned into pET15b	This study
Escherichia coli DH5α p.*oxyR*.ET15B	Cloning strain for *oxyR* cloned into pET15b	This study
Escherichia coli BL21(DE3) p.*oxyRC202S*.ET15B	Protein-expressing strain for OxyR C202S cloned into pET15b	This study
Escherichia coli DH5α p.*oxyRC202S*.ET15B	Cloning strain for *oxyR C202S* cloned into pET15b	This study
Acinetobacter baumannii AB5075	Wild-type parental strain for transposon library	38
Acinetobacter baumannii AB07598	AB5075 transposon mutant *ABUW_2905*-184::T26	38
Acinetobacter baumannii AB07599	AB5075 transposon mutant *ABUW_2905*-143::T26	38
Acinetobacter baumannii AB07600	AB5075 transposon mutant *ABUW_2905*-146::T26	38
Acinetobacter baumannii AB07601	AB5075 transposon mutant *ABUW_2905*-156::T26	38

the presence of H_2O_2 than that *oxyR* deletion strain alone. We expect that the OxyR C202S strain is "locked" in the reduced form, as was demonstrated previously for *E. coli* OxyR C199S (22, 61). Therefore, the presence of reduced OxyR appears to have a detrimental impact on *A. baumannii* growth in the presence of H_2O_2. Since OxyR C202S is capable of DNA binding, we hypothesize that this mutant causes dysregulated expression of the OxyR regulon in the presence of H_2O_2, leading to impaired growth.

Finally, we report that *oxyR* increases the fitness of *A. baumannii* in a murine pneumonia model. Importantly, this result corroborates the imaging data, demonstrating that H_2O_2 is produced *in vivo* during *A. baumannii* infection. The finding that *oxyR* contributes to *A. baumannii* pathogenesis builds on work with *P. aeruginosa*, *E. coli*, *Francisella tularensis*, *Klebsiella pneumoniae*, and *Bacteroides fragilis* demonstrating that *oxyR* mutants are less fit than the WT *in vivo* (62–66). These results define *oxyR* as a factor in *A. baumannii* that is important for fitness during infection, and they contribute to understanding the pathogenesis of this organism, a critical multidrug-resistant threat to human health.

MATERIALS AND METHODS

Bacterial strains and reagents. The strains used in this study are described in Table 4. Unless otherwise noted, all strains are derivatives of the human clinical isolate *A. baumannii* ATCC 17978. Transposon mutants in the *A. baumannii* AB5075 background were purchased from the University of Washington *A. baumannii* mutant library (38). Transposon insertion sites were confirmed by PCR amplification between transposon-specific primer Pgro-172 and primers external to the *oxyR* allele (ERG19 for 5′ and ERG24 for 3′) (see Table S1 in the supplemental material). Cloning was performed in *E. coli* DH5α. Bacteria were routinely grown in lysogeny broth (LB) at 37°C unless otherwise noted. Solid medium contained 1.5% agar. Antibiotics were added at the following concentrations: 75 μg ml^{-1} carbenicillin and 40 μg ml^{-1} kanamycin. All antibiotics were purchased from Sigma (St. Louis, MO).

Strain generation. The primers used in this study are listed in Table S1 in the supplemental material. The in-frame deletion Δ*oxyR* strain was generated via one-step recombineering as described previously (33). Briefly, the *aph1* kanamycin resistance cassette from pUC18K1 was amplified using primer pairs LEJ_209 and LEJ_220, which contained 120-bp regions of homology flanking the *oxyR* open reading frame (ORF). The PCR product was purified using column PCR purification (Qiagen, Hilden, Germany), concentrated to >1 μg/μl, and electroporated into WT *A. baumannii* containing pAT02 (33). Rec_{Ab} expression was induced with 2 mM isopropyl β-D-1-thiogalactopyranoxide (IPTG), cultures were grown at 37°C for 4 h, and half of the transformed cells were plated onto LB agar containing kanamycin. Kanamycin-resistant colonies were restreaked onto LB agar with kanamycin and were screened by PCR for replacement of the *oxyR* allele with *aph1* by use of primer pairs LEJ_213 and LEJ_214. Clones with the correct insertion were restreaked to solid medium containing kanamycin or carbenicillin to screen for the loss of the pAT02 plasmid. Kan^r $Carb^S$ clones were saved at −80°C. The *oxyR* complementation vectors were constructed in pWH1266 under the control of the 16S rRNA promoter (*r01*) by PCR amplification of

the ORF, double digestion of the vector and PCR product with BamHI-HF and SalI-HF (New England Biolabs, Ipswich, MA), and ligation with T4 DNA ligase (Promega, Madison WI). Site-directed mutagenesis was performed by subcloning the *oxyR* ORF into pCR-Blunt (Invitrogen, Carlsbad, CA) and amplifying the vector with *Pfu* Turbo polymerase (Thermo Fisher, Waltham, MA) using primer pairs LEJ_236 and LEJ_237. The 50-μl PCR product was treated with 1.5 μl DpnI (New England Biolabs, Ipswich, MA) for 2 h and was transformed into DH5α, and transformants were plated onto LB agar containing kanamycin. Clones that contained the desired mutations were confirmed by Sanger sequencing, plasmids were miniprepped and digested, and inserts were subcloned into pP_{rot}WH1266 to generate complementation vectors with the desired point mutations.

H_2O_2 growth assays. LB was used as the growth medium for all assays and contained antibiotics as necessary for the maintenance of plasmids. Bacterial strains were freshly streaked onto solid agar and grown to stationary phase in 3-ml overnight cultures. Overnight cultures were subcultured 1:50 in LB for 1 h prior to 1:100 inoculation of medium containing H_2O_2 (30%; EMD Millipore, Darmstadt, Germany) at the concentrations indicated in the figures. All growth assays were carried out in 96-well plates in a 100-μl volume, and growth was measured by optical density at 600 nm (OD_{600}).

H_2O_2 disc diffusion assays. Disc diffusion assays were modified from published protocols (63, 67). Freshly streaked strains were grown to stationary phase in 3-ml overnight cultures and were diluted 1:10 in LB, and 100 μl of diluted culture was added to 4 ml of melted soft agar (0.75% agar) and immediately poured onto LB agar plates, which were allowed to dry for 5 min. Sterile 6-mm paper discs were placed on the center of the plate and were loaded with 10 μl of 9.8 M H_2O_2 (30% H_2O_2; EMD Millipore, Darmstadt, Germany). After incubation at 37°C for 20 h, the zone of growth inhibition was determined as the mean of three separate diameter measurements.

H_2O_2 killing assays. Biological-triplicate overnight cultures of WT *A. baumannii* and the Δ*oxyR* strain were diluted 1:1,000 into 10 ml LB in 50-ml conical tubes and were grown to mid-exponential phase. Cultures were treated with various concentrations of H_2O_2 (EMD Millipore, Darmstadt, Germany) ranging from 1 to 40 mM for 10 or 30 min. At each time point, 10 μl of culture was collected, serially diluted in PBS containing catalase (2,000 U/ml, catalase from bovine liver; Sigma, St. Louis, MO), and spot-plated onto LB agar for CFU enumeration.

OxyR protein alignment. The primary amino acid sequences of selected OxyR orthologues were downloaded from ncbi.gov. Multiple sequence alignment was performed using ClustalOmega on the EBI Web server, which can be found at https://www.ebi.ac.uk/Tools/msa/clustalo/ (68).

OxyR phylogenetic tree. Phylogenetic tree analysis was performed on the Phylogeny.fr platform (69). Sequences were aligned with MUSCLE (v3.8.31) using default settings (70). After alignment, ambiguous regions were removed with Gblocks (v0.91b) (71) with the following settings: a minimum block length of 10, no gap positions allowed, a maximum contiguous segment of nonconserved positions of 8, and a minimum number of sequences for a flank position of 85%. The phylogenetic tree was reconstructed using the maximum likelihood method implemented in the PhyML program (v3.1/3.0, approximate likelihood-ratio test [aLRT]) (72, 73) using the following settings: WAG model, aLRT statistical test, 4 categories, estimated gamma, and estimated invariable sites. Graphical representation of the phylogenetic tree was performed with TreeDyn (v198.3) (74) using the following settings: rectangular conformation, legend displayed, and bootstrap branch annotation.

Purification of recombinant protein. The *oxyR* ORF was cloned into pET15b (Novagen, EMD Millipore, Darmstadt, Germany) to generate N-terminal hexahistidine-tagged constructs. The WT *oxyR* ORF was amplified by primer pair LEJ_227 and LEJ_228, double digested with NdeI and BamHI-HF (New England Biolabs, Ipswich, MA), ligated into pET15b with T4 DNA ligase (Promega, Madison, WI), and transformed into DH5α. The OxyR C202S ORF was cloned by PCR amplification of the ORF from miniprepped plasmid p.*oxyR* C202S using primer pairs LEJ_227 and LEJ_228 and ligation into pCR-Blunt. Digestion and ligation were performed as described for WT *oxyR*. *E. coli* BL21(DE3) was transformed with the resultant vector and was grown at 37°C to an OD_{600} of 0.4 to 0.6 before induction with 1 mM IPTG (Sigma, St. Louis, MO). Following induction, bacteria were maintained at 30°C for an additional 8 to 10 h. Cells were harvested by centrifugation at 6,000 $\times$ *g* for 10 min, washed once with LB, and stored at −70°C. Cells were thawed, resuspended in lysis buffer (50 mM Tris [pH 8], 300 mM NaCl, 20 mM imidazole, 1 mg/ml lysozyme, protease inhibitor cocktail [Sigma, St. Louis, MO], and DNase [Sigma, St. Louis, MO]), Dounce homogenized, and lysed at 20,000 lb/in^2 for 5 min in an EmulsiFlex homogenizer (Aventin, Inc., Ottawa, ON, Canada). Following disruption, lysates were centrifuged at 15,000 rpm for 1 h at 4°C to remove the insoluble fraction. The supernatants were passed through a 45-μm filter and were applied to a Ni-nitrilotriacetic acid (NTA) column (Qiagen, Hilden, Germany). The column was washed with 20 bed volumes of wash buffer (50 mM Tris [pH 8], 300 mM NaCl, 25 mM imidazole) followed by sequential washes with increasing concentrations of imidazole (100 mM, 150 mM, 200 mM, 250 mM, 300 mM, 500 mM). OxyR eluted free of contaminating proteins at 200 mM imidazole. Buffer exchange was performed using PD-10 desalting columns (GE Healthcare Life Sciences, Little Chalfont, UK) to the final buffer (20 mM Tris [pH 8], 500 mM NaCl, 5% glycerol, 10 mM dithiothreitol). The OxyR C202S protein was purified using the same protocol as that for WT OxyR.

Electromobility shift assays. Promoter DNA was amplified by PCR using the primer pairs outlined in Table S1 in the supplemental material and was purified by a Qiagen PCR cleanup kit (Qiagen, Hilden, Germany). Forty nanograms of promoter was incubated for 30 min at room temperature with freshly purified OxyR or OxyR C202S at the concentrations indicated in the figures in EMSA binding buffer (20 mM Tris HCl [pH 7.5], 2.5 mM $MgCl_2$, 0.45 mM EDTA, 0.05% Nonidet P-40, 10% glycerol, and 5 mM dithiothreitol) that was modified with H_2O_2 as noted in Fig. 6. The molarity of promoters in final solution was 13.5 nM for *A1S_1201* (*ahpF1*), 16.4 nM for *A1S_3382* (*katE*), and 10 nM for *mumT*. Samples were

separated by electrophoresis in 6% polyacrylamide-0.5× Tris-buffered EDTA (TBE) gels (5× TBE contained 89 mM Tris base, 89 mM boric acid, and 1 mM EDTA) that were prerun at 100 V for 20 min. Following electrophoresis, gels were stained with SYBR green (Invitrogen, Carlsbad, CA) diluted 1:10,000 in 0.5× TBE for 20 min in the dark, washed twice with H_2O, and visualized with a gel imager (Bio-Rad, Hercules, CA).

Mouse infections. A murine competitive infection model of pneumonia was utilized. Wild-type *A. baumannii* and the isogenic, kanamycin-marked Δ*oxyR* strain were freshly streaked from frozen stocks onto LB agar or LB agar containing 40 μg ml^{-1} kanamycin, respectively, 2 days prior to infection. Overnight cultures were grown in LB without antibiotic selection. On the day of the infection, overnight cultures were subcultured 1:1,000 in 10 ml of LB and were grown to mid-exponential phase. Cells were then harvested by centrifugation, washed twice in PBS, and resuspended in PBS to a final concentration of 1×10^{10} CFU ml^{-1}. Suspensions of wild-type *A. baumannii* and the Δ*oxyR* strain were then combined in a 1:1 ratio, mixed thoroughly, and immediately utilized for infection. Mice were anesthetized by intraperitoneal injection of 2,2,2-tribromoethanol diluted in PBS. Anesthetized mice were inoculated intranasally with 5×10^8 CFU in a 45-μl volume. Infection proceeded for 36 h. Mice were then euthanized with CO_2, and lungs and livers were removed and placed on ice. Organs were homogenized in 1 ml PBS, serially diluted in PBS with catalase (2,000 U/ml; catalase from bovine liver; Sigma, St. Louis, MO), and dilutions were spot-plated onto LB agar and LB agar containing 40 μg ml^{-1} kanamycin. Isogenic mutant burdens were enumerated by counting colonies recovered on kanamycin-containing plates. Infections were performed at the Vanderbilt University Medical Center under the principles and guidelines described in the *Guide for the Care and Use of Laboratory Animals* (75) using Institutional Animal Care and Use Committee (IACUC)-approved protocol M1600123-00. The Vanderbilt University Medical Center is an American Association for Laboratory Animal Science (AALAS)-accredited facility and is registered with the Office of Laboratory Animal Welfare (OLAW), assurance number A-3227-01.

Imaging of H_2O_2 production *in vivo*. Imaging was carried out similarly to published methods (35). FVB-luc$^+$ [FVB-Tg(CAG-luc-GFP)L2G85Chco/J] mice were infected using the protocol described above with WT *A. baumannii*. FVB-luc$^+$ mice were purchased from The Jackson Laboratory (stock no. 008450) and were bred in-house at Vanderbilt University. After 36 h of infection, mice were injected intraperitoneally with 0.05 μmol of Peroxy Caged Luciferin-2 (PCL-2) and 0.05 μmol of D-cysteine in 50 μl dimethyl sulfoxide (DMSO; Sigma, St. Louis, MO). Chemical probes were provided by Chris Chang (UC Berkeley). Mice were imaged 30 min postinjection using a Xenogen IVIS 200 system (Caliper Life Sciences, Hopkinton, MA). Mice were anesthetized prior to injection and during imaging via inhalation of isoflurane (Piramal, Bethlehem, PA). Infections were performed at the Vanderbilt University Medical Center under the principles and guidelines described in the *Guide for the Care and Use of Laboratory Animals* (75) using IACUC-approved protocol M/14/243.

Growth for RNA-seq and RNA isolation. Biological-triplicate overnight cultures of WT *A. baumannii* and the Δ*oxyR* strain were diluted 1:1,000 into 10 ml LB in 50-ml conical tubes and were grown to mid-exponential phase. Cultures were treated with 5.65 μl of 30% H_2O_2 (EMD Millipore, Darmstadt, Germany), for a final concentration of 5 mM, or were left untreated, at 37°C with shaking at 180 rpm for 10 min. Following treatment, 10 μl of bacterial culture was saved for CFU plating, while the remaining bacterial culture was immediately mixed with 10 ml of a 1:1 mixture of ice-cold acetone (JT Baker, Center Valley, PA) and ethanol (Sigma, St. Louis, MO), and the mixture was frozen at −70°C. CFU were enumerated by serially diluting cultures in PBS containing catalase (2,000 U/ml; catalase from bovine liver; Sigma, St. Louis, MO) and spot-plating to LB agar. For RNA purification, thawed cell suspensions were centrifuged at 7,000 rpm for 10 min, supernatants were decanted, and pellets were dried on paper towels. Pellets were resuspended in LETS buffer (0.1 M LiCl, 10 mM EDTA, 10 mM Tris HCl [pH 7.4], 1% SDS), homogenized in a bead beater (Fastprep-24; MP Biomedicals, Santa Ana, CA) with Lysing Matrix B beads (MP Biomedicals, Santa Ana, CA) at a speed of 6 m/s for 45 s, heated at 55°C for 5 min, and centrifuged for 10 min at 15,000 rpm. The upper phase was collected, mixed with 1 ml TRI reagent (Sigma, St. Louis, MO), and incubated for 5 min at room temperature. Chloroform (0.2 ml; Acros Organics, Waltham, MA) was added, samples were vigorously shaken for 15 s, and samples were incubated at room temperature for 2 min. Following centrifugation at 4°C for 15 min, 600 μl of the upper aqueous phase was collected, and RNA was precipitated with 1 ml isopropanol (Sigma, St. Louis, MO). RNA was washed with 70% ethanol (Sigma, St. Louis, MO) and resuspended in 100 μl DNase-free, RNase-free water (Thermo Fisher, Waltham, MA). DNA contamination was removed by treatment with 8 μl RQ1 enzyme (Promega, Madison, WI), 12 μl 10× RQ1 buffer, and 2 μl RiboLock RNase inhibitor (Thermo Fisher, Waltham, MA) for 2 h at 37°C. DNase was removed and samples further purified by the RNeasy kit (Qiagen, Hilden, Germany) according to the manufacturer's instructions, and RNA was stored long-term at −80°C. Each biological replicate was submitted for sequencing without technical replicates.

RNA-seq library preparation and sequencing. RNA-seq library construction and sequencing were performed by HudsonAlpha (Huntsville, AL). The concentration and integrity of the total RNA were estimated with a Qubit 2.0 fluorometer (Invitrogen, Carlsbad, CA) and an Agilent 2100 bioanalyzer (Applied Biosystems, Carlsbad, CA), respectively. Five hundred nanograms of total RNA was required for proceeding to downstream RNA-seq applications. First, rRNA was removed using a Ribo-Zero Gold (Epidemiology) kit (Illumina, San Diego, CA) according to the manufacturer's recommended protocol. Immediately after the rRNA removal, the RNA was fragmented and primed for the first-strand synthesis using the NEBNext First Strand synthesis module (New England Biolabs, Inc., Ipswich, MA). Directional second-strand synthesis was performed using a NEBNext Ultra Directional second-strand synthesis kit. Following this, the samples underwent a standard library preparation protocol using the NEBNext DNA Library Prep Master Mix Set for Illumina with slight modifications. Briefly, end-repair was done followed

by poly(A) addition and custom adapter ligation. Postligated materials were individually barcoded with unique in-house Genomic Services Lab (GSL) primers and were amplified through 12 cycles of PCR. The library quantity was assessed with a Qubit 2.0 fluorometer, and the library quality was estimated by utilizing a DNA High Sense chip on a Caliper Gx system (Perkin-Elmer). Accurate quantification of the final libraries for sequencing applications was determined using the qPCR-based Kapa Biosystems Library Quantification kit (Kapa Biosystems, Inc., Woburn, MA). Each library was diluted to a final concentration of 12.5 nM and pooled in equimolar amounts prior to clustering. Paired-end (PE) sequencing was performed on an Illumina HiSeq 2500 sequencer (Illumina, Inc.).

Processing of RNA-seq reads. RNA-seq analysis was performed by HudsonAlpha (Huntsville, AL). Approximately 25 million 100-bp PE reads were generated from each sample. Further downstream analysis of the sequenced reads from each sample was performed as per the HudsonAlpha unique in-house pipeline. Briefly, quality control checks on raw sequence data from each sample were performed using FastQC (Babraham Bioinformatics, London, UK). Raw reads were imported onto the commercial data analysis platform Avadis NGS (Strand Scientifics, CA, USA) and were mapped to the *A. baumannii* ATCC 17978 reference genome. After quality inspection, the aligned reads were filtered on the basis of read quality metrics, where reads with a base quality score less than 30, an alignment score less than 95, and a mapping quality less than 40 were removed. The remaining reads were then filtered on the basis of their read statistics, where missing mates and translocated, unaligned, and flipped reads were removed. The read list was then filtered to remove duplicates. Samples were grouped, and transcript abundance was quantified on this final read list using Trimmed Means of M-values (TMM) (76) as the normalization method. Differential expression of genes was calculated on the basis of the fold change (using a default cutoff greater than or equal to ± 2.0) observed between defined conditions, and the *P* value of the differentially expressed gene list was estimated by Z-score calculations using by a Benjamini-Hochberg false-discovery-rate (FDR) correction of 0.05 (77).

Quantitative RT-PCR. Two micrograms of RNA was reverse transcribed by Moloney murine leukemia virus (M-MLV) reverse transcriptase (Fisher Scientific, Waltham, MA) in the presence of random hexamers (Promega, Madison, WI) and RiboLock RNase inhibitor (Thermo Fisher, Waltham, MA). Reaction mixtures containing no reverse transcriptase were used to control for DNA contamination. The resultant cDNA was diluted 1:100 and was subjected to qRT-PCR using iQ SYBR green supermix (Bio-Rad, Hercules, CA) with the primer pairs listed in Table S1 in the supplemental material. Amplification was performed on a CFX96 qPCR cycler (Bio-Rad, Hercules, CA) using a 3-step melt curve program. Threshold cycle (C_T) values for each transcript were normalized by 16S rRNA, and fold changes were calculated using the $\Delta\Delta C_T$ method.

Statistical analyses. All raw numerical data were saved in Excel files and imported into GraphPad Prism for statistical analysis. The specific statistical tests employed in each experiment are outlined in the figure legends.

Availability of data and materials. Any materials and data will be made available to members of the scientific community upon communication with the corresponding author.

Accession number(s). Raw RNA sequencing data and processed data are deposited in the NCBI GEO under accession number GSE114130.

SUPPLEMENTAL MATERIAL

Supplemental material for this article may be found at https://doi.org/10.1128/IAI.00413-18.

SUPPLEMENTAL FILE 1, PDF file, 0.7 MB.

ACKNOWLEDGMENTS

L.J.J. conceived of the project, performed experiments, and wrote the manuscript. E.P.S. supervised all studies and helped to write the manuscript. E.R.G. carried out EMSAs. Z.R.L. performed the bioluminescent experiment. C.J.C. and M.C.H. provided the bioluminescent probe.

We thank members of the Skaar laboratory for reviewing the manuscript and Joe Zackular for uploading the RNA-Seq data to GEO.

Work in E.P.S.'s laboratory was supported by Public Health Service grants AI101171, AI069233, and AI073843 and the Defense Advanced Research Projects Agency (DARPA). L.J.J. was supported by American Heart Association grant 15PRE25060007 and Public Health Service award T32 GM07347 from the National Institute of General Medical Studies for the Vanderbilt Medical-Scientist Training Program. L.J.J. is a P.E.O. Scholar. E.R.G. was supported by training grant T32HL094296. Z.R.L. was supported by T32 ES007028 and F31 AI136255. We thank the NIH for grant support of C.J.C. (GM79465). C.J.C. is an Investigator with the Howard Hughes Medical Institute. M.C.H. thanks the University of California President's Postdoctoral Program for postdoctoral fellowship support.

We declare that no conflicts of interest exist.

REFERENCES

1. Dijkshoorn L, Nemec A, Seifert H. 2007. An increasing threat in hospitals: multidrug-resistant *Acinetobacter baumannii*. Nat Rev Microbiol 5:939–951. https://doi.org/10.1038/nrmicro1789.
2. Wong D, Nielsen TB, Bonomo RA, Pantapalangkoor P, Luna B, Spellberg B. 2017. Clinical and pathophysiological overview of *Acinetobacter* infections: a century of challenges. Clin Microbiol Rev 30:409–447. https://doi.org/10.1128/CMR.00058-16.
3. Antunes LC, Visca P, Towner KJ. 2014. *Acinetobacter baumannii:* evolution of a global pathogen. Pathog Dis 71:292–301. https://doi.org/10.1111/2049-632X.12125.
4. Peleg AY, Seifert H, Paterson DL. 2008. *Acinetobacter baumannii*: emergence of a successful pathogen. Clin Microbiol Rev 21:538–582. https://doi.org/10.1128/CMR.00058-07.
5. Perez F, Hujer AM, Hujer KM, Decker BK, Rather PN, Bonomo RA. 2007. Global challenge of multidrug-resistant *Acinetobacter baumannii*. Antimicrob Agents Chemother 51:3471–3484. https://doi.org/10.1128/AAC.01464-06.
6. Potron A, Poirel L, Nordmann P. 2015. Emerging broad-spectrum resistance in *Pseudomonas aeruginosa* and *Acinetobacter baumannii*: mechanisms and epidemiology. Int J Antimicrob Agents 45:568–585. https://doi.org/10.1016/j.ijantimicag.2015.03.001.
7. Giammanco A, Cala C, Fasciana T, Dowzicky MJ. 2017. Global assessment of the activity of tigecycline against multidrug-resistant Gram-negative pathogens between 2004 and 2014 as part of the tigecycline evaluation and surveillance trial. mSphere 2:e00310-16. https://doi.org/10.1128/mSphere.00310-16.
8. World Health Organization. 2017. Global priority list of antibiotic-resistant bacteria to guide research, discovery, and development of new antibiotics. http://www.who.int/medicines/publications/WHO-PPL-Short_Summary_25Feb-ET_NM_WHO.pdf.
9. Harding CM, Hennon SW, Feldman MF. 2018. Uncovering the mechanisms of *Acinetobacter baumannii* virulence. Nat Rev Microbiol 16:91–102. https://doi.org/10.1038/nrmicro.2017.148.
10. McConnell MJ, Actis L, Pachon J. 2013. *Acinetobacter baumannii:* human infections, factors contributing to pathogenesis and animal models. FEMS Microbiol Rev 37:130–155. https://doi.org/10.1111/j.1574-6976.2012.00344.x.
11. Roca I, Espinal P, Vila-Farrés X, Vila J. 2012. The *Acinetobacter baumannii* oxymoron: commensal hospital dweller turned pan-drug-resistant menace. Front Microbiol 3:148. https://doi.org/10.3389/fmicb.2012.00148.
12. Hampton MB, Kettle AJ, Winterbourn CC. 1998. Inside the neutrophil phagosome: oxidants, myeloperoxidase, and bacterial killing. Blood 92:3007–3017.
13. Qiu H, Kuolee R, Harris G, Chen W. 2009. Role of NADPH phagocyte oxidase in host defense against acute respiratory *Acinetobacter baumannii* infection in mice. Infect Immun 77:1015–1021. https://doi.org/10.1128/IAI.01029-08.
14. Demple B. 1991. Regulation of bacterial oxidative stress genes. Annu Rev Genet 25:315–337. https://doi.org/10.1146/annurev.ge.25.120191.001531.
15. Imlay JA. 2013. The molecular mechanisms and physiological consequences of oxidative stress: lessons from a model bacterium. Nat Rev Microbiol 11:443–454. https://doi.org/10.1038/nrmicro3032.
16. Elhosseiny NM, Amin MA, Yassin AS, Attia AS. 2015. *Acinetobacter baumannii* universal stress protein A plays a pivotal role in stress response and is essential for pneumonia and sepsis pathogenesis. Int J Med Microbiol 305:114–123. https://doi.org/10.1016/j.ijmm.2014.11.008.
17. Sun D, Crowell SA, Harding CM, De Silva PM, Harrison A, Fernando DM, Mason KM, Santana E, Loewen PC, Kumar A, Liu Y. 2016. KatG and KatE confer *Acinetobacter* resistance to hydrogen peroxide but sensitize bacteria to killing by phagocytic respiratory burst. Life Sci 148:31–40. https://doi.org/10.1016/j.lfs.2016.02.015.
18. Christman MF, Morgan RW, Jacobson FS, Ames BN. 1985. Positive control of a regulon for defenses against oxidative stress and some heat-shock proteins in *Salmonella typhimurium*. Cell 41:753–762. https://doi.org/10.1016/S0092-8674(85)80056-8.
19. Tao K, Makino K, Yonei S, Nakata A, Shinagawa H. 1991. Purification and characterization of the *Escherichia coli* OxyR protein, the positive regulator for a hydrogen peroxide-inducible regulon. J Biochem 109:262–266.
20. Christman MF, Storz G, Ames BN. 1989. OxyR, a positive regulator of hydrogen peroxide-inducible genes in *Escherichia coli* and *Salmonella typhimurium*, is homologous to a family of bacterial regulatory proteins. Proc Natl Acad Sci U S A 86:3484–3488. https://doi.org/10.1073/pnas.86.10.3484.
21. Chiang SM, Schellhorn HE. 2012. Regulators of oxidative stress response genes in *Escherichia coli* and their functional conservation in bacteria. Arch Biochem Biophys 525:161–169. https://doi.org/10.1016/j.abb.2012.02.007.
22. Choi H, Kim S, Mukhopadhyay P, Cho S, Woo J, Storz G, Ryu SE. 2001. Structural basis of the redox switch in the OxyR transcription factor. Cell 105:103–113. https://doi.org/10.1016/S0092-8674(01)00300-2.
23. Jo I, Chung IY, Bae HW, Kim JS, Song S, Cho YH, Ha NC. 2015. Structural details of the OxyR peroxide-sensing mechanism. Proc Natl Acad Sci U S A 112:6443–6448. https://doi.org/10.1073/pnas.1424495112.
24. Storz G, Tartaglia LA, Ames BN. 1990. Transcriptional regulator of oxidative stress-inducible genes: direct activation by oxidation. Science 248:189–194. https://doi.org/10.1126/science.2183352.
25. Zheng M, Aslund F, Storz G. 1998. Activation of the OxyR transcription factor by reversible disulfide bond formation. Science 279:1718–1721. https://doi.org/10.1126/science.279.5357.1718.
26. Tartaglia LA, Storz G, Ames BN. 1989. Identification and molecular analysis of *oxyR*-regulated promoters important for the bacterial adaptation to oxidative stress. J Mol Biol 210:709–719. https://doi.org/10.1016/0022-2836(89)90104-6.
27. Milse J, Petri K, Ruckert C, Kalinowski J. 2014. Transcriptional response of *Corynebacterium glutamicum* ATCC 13032 to hydrogen peroxide stress and characterization of the OxyR regulon. J Biotechnol 190:40–54. https://doi.org/10.1016/j.jbiotec.2014.07.452.
28. Kim JA, Mayfield J. 2000. Identification of *Brucella abortus* OxyR and its role in control of catalase expression. J Bacteriol 182:5631–5633. https://doi.org/10.1128/JB.182.19.5631-5633.2000.
29. Mongkolsuk S, Sukchawalit R, Loprasert S, Praituan W, Upaichit A. 1998. Construction and physiological analysis of a *Xanthomonas* mutant to examine the role of the *oxyR* gene in oxidant-induced protection against peroxide killing. J Bacteriol 180:3988–3991.
30. Ieva R, Roncarati D, Metruccio MM, Seib KL, Scarlato V, Delany I. 2008. OxyR tightly regulates catalase expression in *Neisseria meningitidis* through both repression and activation mechanisms. Mol Microbiol 70:1152–1165. https://doi.org/10.1111/j.1365-2958.2008.06468.x.
31. Longkumer T, Parthasarathy S, Vemuri SG, Siddavattam D. 2014. OxyR-dependent expression of a novel glutathione S-transferase (Abgst01) gene in *Acinetobacter baumannii* DS002 and its role in biotransformation of organophosphate insecticides. Microbiology 160:102–112. https://doi.org/10.1099/mic.0.070664-0.
32. Geissdorfer W, Kok RG, Ratajczak A, Hellingwerf KJ, Hillen W. 1999. The genes *rubA* and *rubB* for alkane degradation in *Acinetobacter* sp. strain ADP1 are in an operon with *estB*, encoding an esterase, and *oxyR*. J Bacteriol 181:4292–4298.
33. Tucker AT, Nowicki EM, Boll JM, Knauf GA, Burdis NC, Trent MS, Davies BW. 2014. Defining gene-phenotype relationships in *Acinetobacter baumannii* through one-step chromosomal gene inactivation. mBio 5:e01313-14. https://doi.org/10.1128/mBio.01313-14.
34. van Faassen H, KuoLee R, Harris G, Zhao X, Conlan JW, Chen W. 2007. Neutrophils play an important role in host resistance to respiratory infection with *Acinetobacter baumannii* in mice. Infect Immun 75:5597–5608. https://doi.org/10.1128/IAI.00762-07.
35. Van de Bittner GC, Bertozzi CR, Chang CJ. 2013. Strategy for dual-analyte luciferin imaging: *in vivo* bioluminescence detection of hydrogen peroxide and caspase activity in a murine model of acute inflammation. J Am Chem Soc 135:1783–1795. https://doi.org/10.1021/ja309078t.
36. Van de Bittner GC, Dubikovskaya EA, Bertozzi CR, Chang CJ. 2010. *In vivo* imaging of hydrogen peroxide production in a murine tumor model with a chemoselective bioluminescent reporter. Proc Natl Acad Sci U S A 107:21316–21321. https://doi.org/10.1073/pnas.1012864107.
37. Imlay JA. 2015. Transcription factors that defend bacteria against reactive oxygen species. Annu Rev Microbiol 69:93–108. https://doi.org/10.1146/annurev-micro-091014-104322.
38. Gallagher LA, Ramage E, Weiss EJ, Radey M, Hayden HS, Held KG, Huse HK, Zurawski DV, Brittnacher MJ, Manoil C. 2015. Resources for genetic and genomic analysis of emerging pathogen *Acinetobacter baumannii*. J Bacteriol 197:2027–2035. https://doi.org/10.1128/JB.00131-15.
39. Wan F, Shi M, Gao H. 2017. Loss of OxyR reduces efficacy of oxygen respiration in *Shewanella oneidensis*. Sci Rep 7:42609. https://doi.org/10.1038/srep42609.
40. Kullik I, Toledano MB, Tartaglia LA, Storz G. 1995. Mutational analysis of

the redox-sensitive transcriptional regulator OxyR: regions important for oxidation and transcriptional activation. J Bacteriol 177:1275–1284. https://doi.org/10.1128/jb.177.5.1275-1284.1995.
41. Arnold DE, Heimall JR. 2017. A review of chronic granulomatous disease. Adv Ther 34:2543–2557. https://doi.org/10.1007/s12325-017-0636-2.
42. Wymann MP, von Tscharner V, Deranleau DA, Baggiolini M. 1987. Chemiluminescence detection of H_2O_2 produced by human neutrophils during the respiratory burst. Anal Biochem 165:371–378. https://doi.org/10.1016/0003-2697(87)90284-3.
43. Nobre LS, Saraiva LM. 2013. Effect of combined oxidative and nitrosative stresses on *Staphylococcus aureus* transcriptome. Appl Microbiol Biotechnol 97:2563–2573. https://doi.org/10.1007/s00253-013-4730-3.
44. Hajaj B, Yesilkaya H, Shafeeq S, Zhi X, Benisty R, Tchalah S, Kuipers OP, Porat N. 2017. CodY regulates thiol peroxidase expression as part of the pneumococcal defense mechanism against H_2O_2 stress. Front Cell Infect Microbiol 7:210. https://doi.org/10.3389/fcimb.2017.00210.
45. Masloboeva N, Reutimann L, Stiefel P, Follador R, Leimer N, Hennecke H, Mesa S, Fischer HM. 2012. Reactive oxygen species-inducible ECF sigma factors of *Bradyrhizobium japonicum*. PLoS One 7:e43421. https://doi.org/10.1371/journal.pone.0043421.
46. Jang HJ, Nde C, Toghrol F, Bentley WE. 2009. Microarray analysis of *Mycobacterium bovis* BCG revealed induction of iron acquisition related genes in response to hydrogen peroxide. Environ Sci Technol 43:9465–9472. https://doi.org/10.1021/es902255q.
47. Voskuil MI, Bartek IL, Visconti K, Schoolnik GK. 2011. The response of *Mycobacterium tuberculosis* to reactive oxygen and nitrogen species. Front Microbiol 2:105. https://doi.org/10.3389/fmicb.2011.00105.
48. Hoopman TC, Liu W, Joslin SN, Pybus C, Brautigam CA, Hansen EJ. 2011. Identification of gene products involved in the oxidative stress response of *Moraxella catarrhalis*. Infect Immun 79:745–755. https://doi.org/10.1128/IAI.01060-10.
49. Harrison A, Ray WC, Baker BD, Armbruster DW, Bakaletz LO, Munson RS, Jr. 2007. The OxyR regulon in nontypeable *Haemophilus influenzae*. J Bacteriol 189:1004–1012. https://doi.org/10.1128/JB.01040-06.
50. Chang W, Small DA, Toghrol F, Bentley WE. 2005. Microarray analysis of *Pseudomonas aeruginosa* reveals induction of pyocin genes in response to hydrogen peroxide. BMC Genomics 6:115. https://doi.org/10.1186/1471-2164-6-115.
51. Schroeter R, Voigt B, Jurgen B, Methling K, Pother DC, Schafer H, Albrecht D, Mostertz J, Mader U, Evers S, Maurer KH, Lalk M, Mascher T, Hecker M, Schweder T. 2011. The peroxide stress response of *Bacillus licheniformis*. Proteomics 11:2851–2866. https://doi.org/10.1002/pmic.201000461.
52. Salunkhe P, Topfer T, Buer J, Tummler B. 2005. Genome-wide transcriptional profiling of the steady-state response of *Pseudomonas aeruginosa* to hydrogen peroxide. J Bacteriol 187:2565–2572. https://doi.org/10.1128/JB.187.8.2565-2572.2005.
53. Zheng M, Wang X, Templeton LJ, Smulski DR, LaRossa RA, Storz G. 2001. DNA microarray-mediated transcriptional profiling of the *Escherichia coli* response to hydrogen peroxide. J Bacteriol 183:4562–4570. https://doi.org/10.1128/JB.183.15.4562-4570.2001.
54. Bhuiyan MS, Ellett F, Murray GL, Kostoulias X, Cerqueira GM, Schulze KE, Mahamad Maifiah MH, Li J, Creek DJ, Lieschke GJ, Peleg AY. 2016. *Acinetobacter baumannii* phenylacetic acid metabolism influences infection outcome through a direct effect on neutrophil chemotaxis. Proc Natl Acad Sci U S A 113:9599–9604. https://doi.org/10.1073/pnas.1523116113.
55. Cerqueira GM, Kostoulias X, Khoo C, Aibinu I, Qu Y, Traven A, Peleg AY. 2014. A global virulence regulator in *Acinetobacter baumannii* and its control of the phenylacetic acid catabolic pathway. J Infect Dis 210:46–55. https://doi.org/10.1093/infdis/jiu024.
56. Ochsner UA, Vasil ML, Alsabbagh E, Parvatiyar K, Hassett DJ. 2000. Role of the *Pseudomonas aeruginosa oxyR-recG* operon in oxidative stress defense and DNA repair: OxyR-dependent regulation of *katB-ankB, ahpB,* and *ahpC-ahpF*. J Bacteriol 182:4533–4544. https://doi.org/10.1128/JB.182.16.4533-4544.2000.
57. Ravindra Kumar S, Imlay JA. 2013. How *Escherichia coli* tolerates profuse hydrogen peroxide formation by a catabolic pathway. J Bacteriol 195:4569–4579. https://doi.org/10.1128/JB.00737-13.
58. Deretic V, Philipp W, Dhandayuthapani S, Mudd MH, Curcic R, Garbe T, Heym B, Via LE, Cole ST. 1995. *Mycobacterium tuberculosis* is a natural mutant with an inactivated oxidative-stress regulatory gene: implications for sensitivity to isoniazid. Mol Microbiol 17:889–900. https://doi.org/10.1111/j.1365-2958.1995.mmi_17050889.x.
59. Wan F, Kong L, Gao H. 2018. Defining the binding determinants of *Shewanella oneidensis* OxyR: implications for the link between the contracted OxyR regulon and adaptation. J Biol Chem 293:4085–4096. https://doi.org/10.1074/jbc.RA117.001530.
60. Loprasert S, Fuangthong M, Whangsuk W, Atichartpongkul S, Mongkolsuk S. 2000. Molecular and physiological analysis of an OxyR-regulated *ahpC* promoter in *Xanthomonas campestris* pv. phaseoli. Mol Microbiol 37:1504–1514. https://doi.org/10.1046/j.1365-2958.2000.02107.x.
61. Toledano MB, Kullik I, Trinh F, Baird PT, Schneider TD, Storz G. 1994. Redox-dependent shift of OxyR-DNA contacts along an extended DNA-binding site: a mechanism for differential promoter selection. Cell 78:897–909. https://doi.org/10.1016/S0092-8674(94)90702-1.
62. Hennequin C, Forestier C. 2009. *oxyR*, a LysR-type regulator involved in *Klebsiella pneumoniae* mucosal and abiotic colonization. Infect Immun 77:5449–5457. https://doi.org/10.1128/IAI.00837-09.
63. Sund CJ, Rocha ER, Tzinabos AO, Wells WG, Gee JM, Reott MA, O'Rourke DP, Smith CJ. 2007. The *Bacteroides fragilis* transcriptome response to oxygen and H_2O_2: the role of OxyR and its effect on survival and virulence. Mol Microbiol 67:129–142. https://doi.org/10.1111/j.1365-2958.2007.06031.x.
64. Ma Z, Russo VC, Rabadi SM, Jen Y, Catlett SV, Bakshi CS, Malik M. 2016. Elucidation of a mechanism of oxidative stress regulation in *Francisella tularensis* live vaccine strain. Mol Microbiol 101:856–878. https://doi.org/10.1111/mmi.13426.
65. Johnson JR, Clabots C, Rosen H. 2006. Effect of inactivation of the global oxidative stress regulator *oxyR* on the colonization ability of *Escherichia coli* O1:K1:H7 in a mouse model of ascending urinary tract infection. Infect Immun 74:461–468. https://doi.org/10.1128/IAI.74.1.461-468.2006.
66. Lau GW, Britigan BE, Hassett DJ. 2005. *Pseudomonas aeruginosa* OxyR is required for full virulence in rodent and insect models of infection and for resistance to human neutrophils. Infect Immun 73:2550–2553. https://doi.org/10.1128/IAI.73.4.2550-2553.2005.
67. LeBlanc JJ, Brassinga AK, Ewann F, Davidson RJ, Hoffman PS. 2008. An ortholog of OxyR in *Legionella pneumophila* is expressed postexponentially and negatively regulates the alkyl hydroperoxide reductase (*ahpC2D*) operon. J Bacteriol 190:3444–3455. https://doi.org/10.1128/JB.00141-08.
68. Sievers F, Wilm A, Dineen D, Gibson TJ, Karplus K, Li W, Lopez R, McWilliam H, Remmert M, Soding J, Thompson JD, Higgins DG. 2011. Fast, scalable generation of high-quality protein multiple sequence alignments using Clustal Omega. Mol Syst Biol 7:539. https://doi.org/10.1038/msb.2011.75.
69. Dereeper A, Guignon V, Blanc G, Audic S, Buffet S, Chevenet F, Dufayard JF, Guindon S, Lefort V, Lescot M, Claverie JM, Gascuel O. 2008. Phylogeny.fr: robust phylogenetic analysis for the non-specialist. Nucleic Acids Res 36:W465–W469. https://doi.org/10.1093/nar/gkn180.
70. Edgar RC. 2004. MUSCLE: multiple sequence alignment with high accuracy and high throughput. Nucleic Acids Res 32:1792–1797. https://doi.org/10.1093/nar/gkh340.
71. Castresana J. 2000. Selection of conserved blocks from multiple alignments for their use in phylogenetic analysis. Mol Biol Evol 17:540–552. https://doi.org/10.1093/oxfordjournals.molbev.a026334.
72. Guindon S, Gascuel O. 2003. A simple, fast, and accurate algorithm to estimate large phylogenies by maximum likelihood. Syst Biol 52:696–704. https://doi.org/10.1080/10635150390235520.
73. Anisimova M, Gascuel O. 2006. Approximate likelihood-ratio test for branches: a fast, accurate, and powerful alternative. Syst Biol 55:539–552. https://doi.org/10.1080/10635150600755453.
74. Chevenet F, Brun C, Banuls AL, Jacq B, Christen R. 2006. TreeDyn: towards dynamic graphics and annotations for analyses of trees. BMC Bioinformatics 7:439. https://doi.org/10.1186/1471-2105-7-439.
75. National Research Council. 2011. Guide for the care and use of laboratory animals, 8th ed. National Academies Press, Washington, DC.
76. Robinson MD, Oshlack A. 2010. A scaling normalization method for differential expression analysis of RNA-seq data. Genome Biol 11:R25. https://doi.org/10.1186/gb-2010-11-3-r25.
77. Benjamini Y, Hochberg Y. 1995. Controlling the false discovery rate: a practical and powerful approach to multiple testing. J Royal Statist Soc Ser B Methodol 57:289–300.
78. Hood MI, Mortensen BL, Moore JL, Zhang Y, Kehl-Fie TE, Sugitani N, Chazin WJ, Caprioli RM, Skaar EP. 2012. Identification of an *Acinetobacter baumannii* zinc acquisition system that facilitates resistance to calprotectin-mediated zinc sequestration. PLoS Pathog 8:e1003068. https://doi.org/10.1371/journal.ppat.1003068.